

**Integrated Ocean Drilling Program  
Expedition 307 Preliminary Report**

**Modern Carbonate Mounds: Porcupine Drilling**

25 April–30 May 2005

Expedition Scientists

## **PUBLISHER'S NOTES**

Material in this publication may be copied without restraint for library, abstract service, educational, or personal research purposes; however, this source should be appropriately acknowledged.

### **Citation:**

Expedition Scientists, 2005. Modern carbonate mounds: Porcupine drilling. *IODP Prel. Rept.*, 307.  
doi:10.2204/iodp.pr.307.2005

### **Distribution:**

Electronic copies of this series may be obtained from the Integrated Ocean Drilling Program (IODP) Publication Services homepage on the World Wide Web at [iodp.tamu.edu/publications](http://iodp.tamu.edu/publications).

This publication was prepared by the Integrated Ocean Drilling Program U.S. Implementing Organization (IODP-USIO): Joint Oceanographic Institutions, Inc., Lamont-Doherty Earth Observatory of Columbia University, and Texas A&M University, as an account of work performed under the international Integrated Ocean Drilling Program, which is managed by IODP Management International (IODP-MI), Inc. Funding for the program is provided by the following agencies:

European Consortium for Ocean Research Drilling (ECORD)

Ministry of Education, Culture, Sports, Science and Technology (MEXT) of Japan

Ministry of Science and Technology (MOST), People's Republic of China

U.S. National Science Foundation (NSF)

## **DISCLAIMER**

Any opinions, findings, and conclusions or recommendations expressed in this publication are those of the author(s) and do not necessarily reflect the views of the participating agencies, IODP Management International, Inc., Joint Oceanographic Institutions, Inc., Lamont-Doherty Earth Observatory of Columbia University, Texas A&M University, or Texas A&M Research Foundation.

The following scientists and personnel were aboard the *JOIDES Resolution* for Expedition 307 of the Integrated Ocean Drilling Program.

## Expedition Scientists

### **Timothy Ferdelman**

#### **Co-Chief Scientist**

Department of Biogeochemistry  
Max-Planck-Institute of Marine Microbiology  
Celsiusstrasse 1  
28359 Bremen  
Germany

[tferdelm@mpi-bremen.de](mailto:tferdelm@mpi-bremen.de)

Work: (49) 421-2028-651

Fax: (49) 421-2028-690

### **Akihiro Kano**

#### **Co-Chief Scientist**

Department of Earth and Planetary Systems Science  
Graduate School of Science  
Hiroshima University  
Kagamiyama 1-3-1  
Higashi-hiroshima, 739-8526  
Japan

[kano@geol.sci.hiroshima-u.ac.jp](mailto:kano@geol.sci.hiroshima-u.ac.jp)

Work: (81) 82-424-6583

Fax: (81) 82-424-0735

### **Trevor Williams**

#### **Staff Scientist**

Borehole Research Group  
Lamont-Doherty Earth Observatory  
of Columbia University  
PO Box 1000, 61 Route 9W  
Palisades NY 10964  
USA

[trevor@ldeo.columbia.edu](mailto:trevor@ldeo.columbia.edu)

Work: (914) 365-8626

Fax: (914) 365-3182

### **Philippe Gaillot**

#### **Logging Staff Scientist**

Center for Deep Earth Exploration (CDEX)  
Japan Agency of Marine-Earth Science  
and Technology

Yokohama Institute for Earth Sciences  
3173-25 Showa-machi, Kanazawa-ku  
Yokohama Kanagawa 236-0001  
Japan

[gaillotp@jamstec.go.jp](mailto:gaillotp@jamstec.go.jp)

Work: (81) 45-778-5818

Fax: (81) 45-778-5704

### **Kohei Abe**

#### **Paleontologist (foraminifers)**

Graduate School of Life and Environmental  
Sciences  
University of Tsukuba  
1-1-1 Tennodai  
Tsukuba 305-8572  
Japan

[abekohei@arsia.geo.tsukuba.ac.jp](mailto:abekohei@arsia.geo.tsukuba.ac.jp)

Work: (81) 29-853-4465

Fax: (81) 29-851-9764

### **Miriam S. Andres**

#### **Sedimentologist**

Rosenstiel School of Marine and Atmospheric  
Science  
University of Miami  
4600 Rickenbacker Causeway  
Miami FL 33149  
USA

[mandres@rsmas.miami.edu](mailto:mandres@rsmas.miami.edu)

Work: (305) 421-4683

Fax: (305) 421-4632

### **Morten Bjerager**

#### **Sedimentologist**

Geologisk Institut  
University of Copenhagen  
Oster Voldgade 10  
1350 Copenhagen  
Denmark

[mortenb@geol.ku.dk](mailto:mortenb@geol.ku.dk)

Work: (45) 3532 2401

Fax: (45) 3314 8322

### **Emily L. Browning**

#### **Paleontologist (nannofossils)**

4019 Sumner Street  
Lincoln NE 68506  
USA

[ebrowning3@hotmail.com](mailto:ebrowning3@hotmail.com)

Work: (251) 554-7756

**Barry A. Cragg**  
**Microbiologist**  
Department of Earth Sciences  
Cardiff University  
Main Building, Park Place  
Cardiff Wales CF10 3YE  
United Kingdom  
[b.cragg@earth.cardiff.ac.uk](mailto:b.cragg@earth.cardiff.ac.uk)  
Work: (44) 29-2087-4928  
Fax: (44) 29-2087-4326

**Ben De Mol**  
**Stratigraphic Correlator**  
GRC Geociències Marines  
Universitat de Barcelona  
Campus de Pedralbes  
08028 Barcelona  
Spain  
[bendemol@ub.edu](mailto:bendemol@ub.edu)  
Work: (34) 93 403 4641  
Fax: (34) 93 402 1340

**Anneleen Foubert**  
**Paleomagnetist**  
Renard Centre of Marine Geology  
Universiteit Gent  
Geology and Soil Sciences  
Krijgslaan 281-S8  
9000 Gent  
Belgium  
[anneleen.Foubert@UGent.be](mailto:anneleen.Foubert@UGent.be)  
Work: (32) 9264 4591  
Fax: (32) 9264 4967

**Tracy D. Frank**  
**Inorganic Geochemist**  
Geosciences Department  
University of Nebraska, Lincoln  
214 Bessey Hall  
Lincoln NE 68588-0340  
USA  
[tfrank2@unl.edu](mailto:tfrank2@unl.edu)  
Work: (402) 472-9799  
Fax: (402) 472-4917

**Yuji Fuwa**  
**Paleomagnetist**  
Department of Earth Sciences  
Toyama University  
Gofuju 3190  
Toyama 930  
Japan  
[m052197@ems.toyama-u.ac.jp](mailto:m052197@ems.toyama-u.ac.jp)  
Work: (81) 076-445-6649  
Fax: (81) 076-445-6549

**Jamshid J. Gharib**  
**Inorganic Geochemist**  
Department of Geology and Geophysics/SOEST  
University of Hawaii at Manoa  
1680 East West Road  
Honolulu HI 96822  
USA  
[gharib@hawaii.edu](mailto:gharib@hawaii.edu)  
Work: (808) 956-8558  
Fax: (808) 956-5512

**Jay M. Gregg**  
**Sedimentologist**  
Geological Sciences and Engineering  
University of Missouri-Rolla  
125 McNutt Hall  
1870 Miner Circle  
Rolla MO 65409  
USA  
[greggjay@umr.edu](mailto:greggjay@umr.edu)  
Work: (573) 241-4664  
Fax: (573) 341-6935

**Veerle Ann Ida Huvenne**  
**Stratigraphic Correlator**  
Challenger Division for Seafloor Processes  
Southampton Oceanography Centre  
Waterfront Campus  
European Way  
Southampton England SO14 3ZH  
United Kingdom  
[vaih@soc.soton.ac.uk](mailto:vaih@soc.soton.ac.uk)  
Work: (44) 23 8059 6263  
Fax: (44) 23 8059 6554

**Philippe Léonide**  
**Organic Geochemist**  
Centre de Sédimentologie-Paléontologie  
Université de Provence  
CNRS Research Unit FRE 2761  
3 Place Victor Hugo, case 67  
13331 Marseille Cedex 03  
France  
[leonide@up.univ-mrs.fr](mailto:leonide@up.univ-mrs.fr)  
Work: (33) 4 91 10 6208  
Fax: (33) 4 91 10 8523

**Xianghui Li**

**Sedimentologist**

Department of Earth Sciences  
Chengdu University of Technology  
Er'xianqiao Dongsanlu  
Chengdu Sichuan 610059  
Peoples Republic of China  
[lixh@cdut.edu.cn](mailto:lixh@cdut.edu.cn)

Work: (86) 28-84079527

Fax: (86) 28-84075588

**Kai Mangelsdorf**

**Microbiologist/Geochemist**

Organic Geochemistry and Hydrocarbon Systems  
Geo Forschungs Zentrum Potsdam  
Department 4.3, Telegrafenberg B423  
14473 Potsdam  
Germany

[k.mangelsdorf@gfz-potsdam.de](mailto:k.mangelsdorf@gfz-potsdam.de)

Work: (49) 331-288-1785

Fax: (49) 331-288-1782

**Akiko Tanaka**

**Physical Properties Specialist**

Institute of Geology and Geoinformation  
Geological Survey of Japan, AIST  
Tsukuba Central 7  
1-1-1 Higashi  
Tsukuba Ibaraki 305-8567  
Japan

[akiko-tanaka@aist.go.jp](mailto:akiko-tanaka@aist.go.jp)

Work: (81) 29-861-3962

Fax: (81) 29-861-3609

**Ivana Novosel**

**Sedimentologist**

Department of Earth Sciences  
Rice University  
6100 Main Street, MS-126  
Houston TX 77005-1892  
USA

[novosel@rice.edu](mailto:novosel@rice.edu)

Work: (713) 348-4135

Fax: (713) 348-5214

**Saburo Sakai**

**Inorganic Geochemist**

Institute for Frontier Research on Earth Evolution  
(IFREE)  
Japan Agency of Marine-Earth Science  
and Technology  
2-15 Natsushima-cho  
Yokosuka 237-0061  
Japan

[saburos@jamstec.go.jp](mailto:saburos@jamstec.go.jp)

Work: (81) 46-867-9784

Fax: (81) 46-867-9775

**Vladimir A. Samarkin**

**Microbiologist**

Department of Marine Sciences  
University of Georgia  
220 Marine Sciences Building  
Athens GA 30601  
USA

[samarkin@uga.edu](mailto:samarkin@uga.edu)

Work: (706) 353-0593

Fax: (706) 542-5888

**Keiichi Sasaki**

**Sedimentologist**

Department of Cultural Properties and Heritages  
Kanazawa Gakuin University  
10 Sue-machi  
Kanazawa Ishikawa 920-1392  
Japan

[sasak1@kanazawa-gu.ac.jp](mailto:sasak1@kanazawa-gu.ac.jp)

Work: (81) 76-229-8859

Fax: (81) 76-229-8718

**Arthur J. Spivack**

**Microbiologist/Geochemist**

Graduate School of Oceanography  
University of Rhode Island  
Marine Geology  
Bay Campus, South Ferry Road  
Narragansett RI 02882  
USA

[spivack@gso.uri.edu](mailto:spivack@gso.uri.edu)

Work: (401) 874-6200

Fax: (401) 874-6811

**Chizuru Takashima**

**Sedimentologist**

Earth and Planetary Systems Science  
Hiroshima University  
Kagamiyama 1-3-1  
Higashi Hiroshima 739-8526  
Japan

[tksmcmdr@hiroshima-u.ac.jp](mailto:tksmcmdr@hiroshima-u.ac.jp)

Work: (81) 824-24-6583

Fax: (81) 824-24-0735

**Jürgen Titschack**

**Sedimentologist**

Institut für Paläontologie  
Universität Erlangen-Nürnberg  
Loewenichstrasse 28  
91054 Erlangen  
Germany

[jurgen.titschack@pal.uni-erlangen.de](mailto:jurgen.titschack@pal.uni-erlangen.de)

Work: (49) 131-852-4756

Fax: (49) 131-852-2690

## Observers

**Boris Dorschel**  
Department of Geology  
University College Cork  
Donovan's Road  
Cork  
Ireland  
[dorschel@uni-bremen.de](mailto:dorschel@uni-bremen.de)

**Xavier Monteys**  
Marine Department  
Geological Survey of Ireland  
Beggars Bush, Haddington Road  
Dublin D4  
Ireland  
[xavier.monteys@gsi.ie](mailto:xavier.monteys@gsi.ie)  
Work: (353) 1604 1466  
Fax: (353) 1604 1436

## Transocean Officials

**Alexander Simpson**  
**Master of the Drilling Vessel**  
Overseas Drilling Ltd.  
707 Texas Avenue South, Suite 213D  
College Station TX 77840-1917  
USA

**Wayne Malone**  
**Drilling Superintendent**  
Overseas Drilling Ltd.  
707 Texas Avenue South, Suite 213D  
College Station TX 77840-1917  
USA

## IODP Shipboard Personnel and Technical Representatives

**Andy Baker**  
Marine Laboratory Specialist: Downhole Tools/  
Thin Sections

**Bill Crawford**  
Imaging Specialist

**Lisa K. Crowder**  
Assistant Laboratory Officer

**Klayton Curtis**  
Marine Laboratory Specialist: Paleomagnetism

**Roy T. Davis**  
Laboratory Officer

**Javier Espinosa**  
Schlumberger Engineer

**David Fackler**  
Applications Developer

**Kazuho Fujine**  
Marine Laboratory Specialist: Core

**Dennis Graham**  
Marine Laboratory Specialist: Chemistry

**Margaret Hastedt**  
Marine Computer Specialist

**Kristin Hillis**  
Yeoperson

**Denise Hudson**  
Laboratory Specialist: Underway Geophysics

**Eric Jackson**  
Marine Laboratory Specialist: X-Ray

**Jan Jurie Kotze**  
Marine Instrumentation Specialist

**David Morley**  
Marine Computer Specialist

**Chieh Peng**  
Assistant Laboratory Officer

**Pieter Pretorius**  
Marine Instrumentation Specialist

**Derryl Schroeder**  
Operations Superintendent

**Paula Weiss**  
Marine Curatorial Specialist

**Brad Weymer**  
Marine Laboratory Specialist: Physical Properties

**Robert M. Wheatley**  
Laboratory Specialist: Chemistry

## ABSTRACT

Challenger Mound, a putative carbonate mound structure covered with dead deepwater coral rubble and located in Porcupine Seabight on the southwest Irish continental margin, was the focal point of twelve days of scientific drilling aboard the *JOIDES Resolution* during Integrated Ocean Drilling Program Expedition 307.

Specific drilling objectives included the following:

1. Establish whether the mound base rested on a carbonate hardground of microbial origin and whether past geofluid migration events acted as a prime trigger for mound genesis.
2. Define the relationship, if any, between mound initiation, mound growth phases, and global oceanographic events.
3. Analyze geochemical and microbiological profiles that define the sequence of microbial communities and geomicrobial reactions throughout the drilled sections.
4. Examine high-resolution paleoclimatic records from the mound section using a wide range of geochemical and isotopic proxies.
5. Describe the stratigraphic, lithologic, and diagenetic characteristics, including timing of key mound-building phases, for establishing a depositional model of deepwater carbonate mounds and for investigating how they resemble ancient mud mounds.

In addition to the mound, one site immediately downslope of Challenger Mound and an upslope site were drilled to (1) constrain the stratigraphic framework of the slope/mound system, (2) identify and correlate erosional surfaces observed in slope sediment seismics, and (3) investigate potential gas accumulation in the sediments underlying the mound.

Drilling revealed that the mound rests on a sharp erosion boundary. Sediments below this erosion surface consist of glauconitic and silty sandstone drift deposits of middle Miocene age that grade upward toward more clay rich intervals. The latter are tentatively interpreted to represent relatively low energy environments in the late Miocene–Pliocene succession. The Pliocene strata end abruptly in a firmground that is overlain by the Pleistocene mound succession. Biostratigraphic results suggest that the hiatus between the two successions spans at least 1.65 m.y. The mound flanks are draped by late Pleistocene (<0.26 Ma) silty clay deposits that frequently contain dropstones.

The mound succession just above the firmground is represented by interbedded grainstone, floatstone, rudstone, packstone, and wackestone in decimeter thicknesses, all reflecting relatively rapidly changing depositional realms. Above this lower level, the mound succession shows pronounced recurring cycles of Pleistocene coral floatstone, rudstone, wackestone, and packstone on a several meter scale that are well represented in the carbonate content change and are most probably associated with Pleistocene glacial–interglacial cycles. A role for hydrocarbon fluid flow in the initial growth phase of Challenger Mound is not obvious either from the lithostratigraphy or from initial geochemistry and microbiology results. We found no significant quantities of gas in the mound or in the subbasal mound sediments, nor were carbonate hardgrounds observed at the mound base.

Microbial effects on mound and submound diagenesis are more subtle. We detected the methane–sulfate transition only in the deeper-lying Miocene silt and sandstones underlying the mound, where methane concentrations and prokaryotic cell abundances increase with increasing depth. In the mound itself, interstitial water profiles of sulfate, alkalinity, Mg, and Sr suggest a tight coupling between carbonate diagenesis and microbial sulfate reduction. Decomposition of organic matter (organoclastic) by sulfate reduction may drive the biogeochemical processes of mineralogical transformation by (1) producing CO<sub>2</sub>, which enhances aragonite dissolution and (2) increasing overall dissolved inorganic carbon concentration, which allows dolomite or high-Mg calcite to precipitate. Furthermore, periods of rapid sedimentation overlying hiatuses apparently left distinct signals in the interstitial water chemistry of the Pleistocene sediments that surround and partially bury the carbonate mounds of Porcupine Seabight.

## INTRODUCTION

Carbonate mounds and reefs are a fundamental and recurrent expression of life in the geological record from Precambrian times onward. The true dawn of carbonate mud mounds is in Cambrian times, when mounds suddenly featured a diversity in microbial and biodetrital fabrics with abundant mound-building calcified microbes (Riding, 1991), calcareous algae, and a variety of Paleozoic benthic invertebrates that may have played an ancillary role in mound construction. In mid- to late Ordovician times, the dramatic rise of large skeletal metazoans such as stromatoporoids, corals (*Rugosa* and *Tabulata*), and bryozoans, as well as higher algae, paved the way for the strong development of reefs and typical stromatoloid mud mounds. Lower Devo-

nian (Gedinnian) mounds in the Montagne Noire, France, exhibit the most spectacular stromatactis fabrics, interpreted as the result of decaying microbial mats (Flajs and Hüssner, 1993). Stratigraphically younger (Emsian) conical carbonate mounds (kess-kess) of the Moroccan Anti-Atlas are related to precipitation from hydrothermal fluids (Kaufmann, 1997), some of which are inferred to be related to a light carbon source (hydrocarbon). Some of the most impressive of early Carboniferous bank aggregates, as thick as 1 km, are those known as the Waulsortian reefs (Lees, 1988; Somerville, 2003). In full Mesozoic times, declines in the abundance and diversity of microbial mounds are recorded from the Triassic to the Cretaceous. From the mid-Cretaceous onward, microbial fabrics are only known as components to metazoan framework reefs (Riding, 1991). Most Cenozoic mud mounds are of biotrital origin, although microbial components might have remained significant in deeper water. Scientific drilling (Ocean Drilling Program [ODP] Leg 182) confirmed the existence of bryozoan reef mounds buried in the cold-water carbonate platform sediments at 200–350 meters below sea level (mbsl) in Great Australian Bight (Feary et al., 1999; James et al., 2000). These mound complexes consist of unlithified floatstone structures, rich in zooidal bryozoan forms that were still growing during the last glacial lowstand.

Coral reefs are commonly considered to have developed in shallow-water tropical to subtropical regions with typical carbonate depositional environments. However, the discovery of large-scale deepwater carbonate mounds extending along the northeastern Atlantic continental margins as well as the Australian bryozoan reef mounds in cool-water slope environments has cast new interest on their structure, origin, and development. The Atlantic coral mounds from depths where light cannot reach were first described by Neuman et al. (1977). They discovered that benthic invertebrates including corals and crinoids construct mounds several hundred meters wide and 50 m high at 600–700 mbsl along the Straits of Florida west of the Bahamas. They were considered to be an exceptional case of coral reefs developed in amazingly deep environments, but contemporaneously similar structures had been recognized in numerous oil industry seismic profiles collected from the northeast Atlantic. Scientific research on deepwater coral mounds was stimulated by the release of some of these profiles in the mid-1990s. Oceanographic exploration using side-scan sonar, underwater video imagery, and drag sampling has collected information on bottom sediments and indicated that the structures are really formed by benthic communities with cold-water corals. Currently, the deepwater coral banks and mounds are known to occur at depths to 1500 m on shelves, shelf margins, and seamounts of the northeast Atlantic from Morocco to Arctic Norway. Additional high-resolution seismic surveys revealed that the mound structures can reach a width of several kilometers (Freiwald et al.,

2004) and a height of 350 m (Kenyon et al., 2003). Exploration for deepwater coral banks was recently expanded outside of Atlantic areas and showed their possible global distribution.

Among the deepwater mound provinces, the most intensively studied provinces are offshore of Norway, Rockall Trough, and Porcupine Seabight located southwest of Ireland. Along the Norwegian continental slope extending from 62°–70°N, cold-water corals form banks or mounds up to 40 m high at 400–500 mbsl. They appear to develop on stable substrate formed of the exposed Neogene sedimentary rock and boulders derived from fjords (Freiwald et al., 1997).

The Porcupine Seabight area surpasses the Norwegian offshore area in terms of size and frequency of the mounds and is the most important Atlantic mound area. Seismic studies have revealed more than 1500 carbonate mounds in the Magellan mound province, and it is estimated that there are ~2000 mounds in Porcupine Basin (De Mol et al., 2002; Huvenne et al., 2003) that generally exhibit conical geometries surrounded or covered by siliciclastic contourites. They can reach as high as 250 m and as wide as 5 km (Huvenne et al., 2002, 2003; De Mol et al., 2002). The mounds in Porcupine Seabight have been the focus of more than 20 cruises in the last decade. Sediments and video images collected on the seafloor indicate that the mounds are commonly colonized by various biota including deep-sea corals *Lophelia* and *Madrepora* and other invertebrates (Foubert et al., 2005). However, details on the internal structure, initiation, and growth of these impressive seafloor features within Porcupine Seabight remained veiled. Explanations of the origin and evolution of the Porcupine mounds revolve around two scenarios that may be expressed as either competing or complementary hypotheses: (1) oceanographic and paleoenvironmental conditions control mound initiation and growth, and (2) hydrocarbon seepage initiates microbial-induced carbonate formation and indirectly fuels coral growth (endogenous control) (Hovland et al., 1998; Henriot et al., 2001). The oceanographic or environmental hypothesis states that the most important conditions stimulating mound development are the interaction of water currents and sediment dynamics. Enhanced currents provide nutrient for the corals and may sweep free stable substrates for settlement of coral larvae (Frederiksen et al., 1992; De Mol et al., 2002 [Porcupine]; Kenyon et al., 2003 [Rockall]; Freiwald et al. 1997 [Norway]; Colman et al., 2005 [Mauritania]). Enhanced bottom currents at tidal frequency (Pingree and Le Cann, 1989, 1990) are observed in the Porcupine mound provinces (Rice et al., 1991). They may result from the internal tides at the boundary between water masses of different densities, such as between Mediterranean Outflow Water (MOW) and Eastern

North Atlantic Water (ENAW), located at ~800 meters below seafloor (mbsf) at present (White, 2001). A strong current provides suspended food to filter-feeding cold-water corals, sweeps the polyps clean of detritus, and protects the corals from sediment burial. Initiation of mound development has been linked to global paleoceanographic change. Closure of the Isthmus of Panama at ~4.6 Ma deviated the huge warm-water mass of ENAW and increased deepwater advection and stratification in the Atlantic (Haug and Tiedemann, 1998). In combination, MOW resumed after the late Miocene–Early Pliocene salinity crisis in the Mediterranean (Maldonado and Nelson, 1999). The oldest fossil records of *Lophelia* and *Madrepora* were reported from the Mediterranean area in the Early Pliocene. Initiation of the deep-sea coral mounds might have been related to establishment of MOW and/or ENAW, which introduced larvae of the cold-water corals to the northeast Atlantic in a manner similar to the coral banks established on the Nordic continental shelf break (Henriet et al., 1998).

The seepage hypothesis was first proposed by Hovland et al. (1994), who correlated the distribution between coral mounds with areas showing high dissolved light hydrocarbon contents in water. Hydrocarbon seepage may prepare favorable conditions for deep-sea corals, in terms of raised inorganic carbon for skeletal accretion (Hovland et al., 1998) and for submarine lithification providing stable substrate. The aligned occurrence seen in some mounds of Porcupine Seabight suggests that the mounds were established along linear structures, such as faults (Hovland et al., 1994). Bailey et al. (2003), however, studied the Magellan mound province in detail from two-dimensional and three-dimensional (3-D) seismic data and found no correlation between mounds and fault locations. Henriet et al. (1998) suggested that conditions in the Magellan province during glacial periods were probably suitable for gas hydrate formation and that decomposition of the gas hydrate could trigger a submarine slide. Later phases of gas seepage would then be focused by this buried slide to specific locations, causing the ringlike structure in the Magellan mounds. The oceanographic and fluid seepage scenarios may have acted in a complementary fashion: microbially induced carbonate hardground formation associated with gas or hydrocarbon seepage provided the hard substrate required by the settling coral larvae. Once established, further development of the mound was subject to oceanographic conditions suitable for further coral growth. The presence of corals covering the mound may be only fortuitous. The mounds themselves may be composed of microbial automicrite, like well-known Phanerozoic carbonate mounds, but only recently covered by cold-water corals. Coral growth might even have led to accelerated burial of the mound structures through enhanced baffling and trapping of sediment. Conclusive evidence for any of these theories is still missing. Only scientific drilling through the core of a mound

structure will provide clearer insight to the formation and development of these enigmatic structures. Integrated Ocean Drilling Program (IODP) Expedition 307 was proposed to obtain evidence for understanding the origin and evolution of the deepwater carbonate mounds in Porcupine Seabight. Sedimentary processes and paleoclimatic history are recorded in lithostratigraphic, biostratigraphic, magnetostratigraphic, and physical property data. In addition, the mounds may be biological constructions associated with hydrocarbon-rich fluids and therefore provide a unique habitat for the deep biosphere. Geochemical and microbiological profiles would define the sequence of microbial communities and geomicrobial reaction throughout the drilled sections and provide basic information to understand diagenetic processes within the mounds.

The Atlantic deep-sea carbonate mounds share geometric features and occurrences with numerous Phanerozoic mud mounds of different ages formed under the control of microbial processes. Perhaps the Porcupine mounds are present-day analogs for the Phanerozoic reef mounds and mud mounds, for which depositional processes and environmental settings are not fully understood. Or are these mounds North Atlantic equivalents to the Quaternary bryozoan mounds found in Great Australian Bight? Limestone bodies that contain coral skeletons are usually interpreted as indicating warm and shallow water; however, the abundance of deepwater coral mounds mean such paleoenvironmental interpretation may not be so simple.

Deepwater coral mounds may also be potential high-resolution environmental recorders. Mound section lithology and bioclastic composition might record glacial–interglacial climate changes because cold-water corals are sensitive to conditions such as water temperature and current strength. Furthermore, coral skeletons themselves can be used for analysis:  $^{14}\text{C}$  and Cd content were used to reconstruct changes in deep-sea circulation (Frank et al., 2004) and nutrient contents (Adkins et al., 1998), respectively. Cold-water corals grow as fast as 25 mm/y (Rogers, 1999), fast enough to apply the same methods of the coral climatology using tropical–subtropical reef-forming corals. Analyses of stable isotopes and trace elements are expected to provide temperature and carbon circulation data at a subannual resolution.

## BACKGROUND

### Overview of Porcupine Seabight Mounds

A geographic overview of Porcupine Seabight and the mound provinces is shown on Figure **F1**. Three different types of mound provinces were identified: the Hovland, Magellan, and Belgica mounds.

#### *Hovland Mounds*

The first mound occurrences reported from industrial data on the northern slope of Porcupine Basin (Hovland et al., 1994) led to the unveiling of a complex setting with large multiphased contourite deposits and high-energy sediment fills, topped by a set of outcropping mounds or elongated mound clusters as high as 250 m (Henriet et al., 1998; De Mol et al., 2002).

#### *Magellan Mounds*

The Hovland mounds are flanked to the north and west by the crescent-shaped, well-delineated Magellan mound province with a very high density of buried medium-sized mounds (1 mound/km<sup>2</sup>; average height = 60–80 m). High-resolution seismic data (Henriet et al., 2001) combined with 3-D industrial seismic data (Huvenne et al., 2003) shed light on the presence of a past slope failure that underlies most of the mound cluster.

#### *Belgica Mounds*

On the eastern margin of Porcupine Basin, a 45 km long range of large mounds towers from a strongly erosional surface (Fig. **F1**). The mounds partly root on an enigmatic, deeply incised, very faintly stratified seismic facies (Unit P2) (De Mol et al., 2002; Van Rooij et al., 2003). De Mol et al. (2002) interpreted this seismic facies as a nannofossil ooze of Pliocene age analogous to the similar seismic facies of ODP Site 980 in the southwestern Rockall Trough (Jansen, Raymo, Blum, et al., 1996) and partly on a layered sequence capped by a surprising set of short-wavelength, sigmoidal depositional units (De Mol et al., 2002; Van Rooij et al., 2003).

The Belgica mound province consists of 66 conical mounds (single or in elongated clusters) in water depths ranging from 550 to 1025 m. The mounds are partly enclosed in an impressive set of contourites (Van Rooij et al., 2003). Mounds typically trap sediment on their upslope flank, which is consequently buried, whereas their

seaward side is well exposed and forms a steep step in bathymetry. Average slopes are 10°–15°. The largest mounds have a height of ~170 m. In the deeper part of the Belgica mound province (Beyer et al., 2003), an extremely “lively” mound was discovered in 1998 on the basis of a very diffuse surface acoustic response. This mound, known as Thérèse Mound, was selected as a special target site to study processes involved in mound development for European Union (EU) Fifth Framework research projects. Video imaging revealed that Thérèse Mound, jointly with its closest neighbor, Galway Mound, might be one of the richest deepwater coral environments in Porcupine Seabight, remarkably in the middle of otherwise barren mounds (Galanes-Alvarez, 2001; Foubert et al., 2005, De Mol et al., in press).

## Geological Setting

Porcupine Seabight forms an inverted triangle opening to the Porcupine Abyssal Plain through a narrow gap of 50 km at a water depth of 2000 m at its southwest apex between the southern and western tips of the Porcupine Bank and terraced Goban Spur, respectively. Porcupine Seabight gradually widens and shoals to depths of 500 m to the east on the Irish continental shelf and north to Slyne Ridge. Porcupine Seabight, which is the surface expression of the underlying deep sedimentary Porcupine Basin (Fig. F2), is a failed rift of the proto-North Atlantic Ocean and is filled with a 10 km thick series of Mesozoic and Cenozoic sediments (Shannon, 1991). Basin evolution can be summarized in three major steps: a Paleozoic synrift phase, a predominantly Jurassic rifting episode, and a Late Cretaceous–Holocene thermal subsidence period.

### *Basin Development and Synrift Sedimentation*

The basement of Porcupine Basin is composed of Precambrian and lower Paleozoic metamorphic rocks forming continental crust ~30 km thick (Johnston et al., 2001). The prerift succession commences with probably Devonian clastic sediments overlain by lower Carboniferous carbonates and clastics. The upper Carboniferous rocks feature deltaic to shallow-marine deposits with Westphalian coal-bearing sandstones and shales and possibly Stephanian redbed sandstones (Shannon, 1991; Moore and Shannon, 1995). The lowermost Mesozoic deposits are early rift valley continental sediments which can be >2 km thick. During Permian times, predominantly fluvial and lacustrine sedimentation took place with nonmarine mixed clastic deposits and evaporites. Triassic sediments contain nonmarine to marine facies (Ziegler, 1982; Shannon, 1991). Lower Jurassic deposits are not found over the entire basin but could comprise limestones and rare organic-rich shales with sandstones.

### *Jurassic Rifting Phase*

The middle Kimmerian rifting phase marked an increase in tectonic events in the Arctic, Atlantic, and Thetys rift systems. This major tectonic event was apparently accompanied by a renewed eustatic lowering of sea level and is likely responsible for erosion of a large part of the Triassic and Jurassic deposits (Ziegler, 1982). Middle Jurassic fluvial claystones and minor sandstones might lie unconformably above earlier deposited strata and can be considered to be products of this major rifting episode. During the Late Jurassic, differential subsidence was responsible for the transition from a continental to a shallow-marine sedimentary environment in Porcupine Basin.

### *Postrift Thermal Subsidence*

At the start of the Cretaceous, the general structure of Porcupine Basin could be compared with a rift structure prior to breakup; its specific failed rift structure has a typical steer's head profile (Moore and Shannon, 1991). A major rifting pulse during the Early Cretaceous, referred to as late Kimmerian tectonics, was accompanied by a significant eustatic sea level fall and gave rise to a regional unconformity that is largely of submarine nature (Ziegler, 1982; Moore and Shannon, 1995). This undulatory unconformity marks the base of the Cretaceous, where marine strata onlap Jurassic sequences (Shannon, 1991). The onset of the Upper Cretaceous was characterized by a further relative sea level rise, featuring offshore sandstone bars, followed by a northward thinning and onlapping outer shelf to slope sequence of carbonates (chalk). Along the southwestern and southeastern margins of the basin, Moore and Shannon (1995) recognized the presence of biohermal reef buildups. The transition from Late Cretaceous to early Paleocene sedimentation is characterized by a high-amplitude seismic reflector marking the change from carbonate to clastic deposition (Shannon, 1991). Most of the Paleogene postrift sediments are dominantly sandstones and shales, influenced by frequent sea level fluctuations. In general, the Paleocene succession is more mud-dominated, whereas the main coarse clastic input occurred in the middle Eocene to earliest late Eocene (McDonnell and Shannon, 2001). The Paleocene–Eocene is subdivided into five sequences characterized by southerly prograding complex deltaic events overlain by marine transgressive deposits (Naylor and Shannon, 1982; Moore and Shannon, 1995). The controls on the relative rises and falls in sea level are dominantly due to the North Atlantic plate tectonic regime. During the late Paleogene and Neogene, passive uplift of the Norwegian, British, and Irish landmasses was very important in shaping the present-day Atlantic margin. Although the origin of this uplift remains unclear, it probably resulted in enhancement of contour

currents, causing local erosion and deposition and an increased probability of sedimentary slides and slumps. Therefore, overall Oligocene and Neogene sedimentation is characterized by along-slope transport and redepositional processes yielding contourite siltstones and mudstones and hemipelagic–pelagic deep-marine sediments, caused by a combination of differential basin subsidence and regional sea level and paleoclimate changes. The youngest unconformity mapped in Porcupine Basin is correlated with an Early Pliocene erosion event in Rockall Basin and is considered to be a nucleation site for present-day coral mounds (McDonnell and Shannon, 2001; De Mol et al., 2002; Van Rooij et al., 2003).

### *Pleistocene and Holocene Sedimentation*

Recent sedimentation is mainly pelagic to hemipelagic, although foraminiferal sands (probably reworked) can be found on the upper slope of the eastern continental margin. The main sediment supply zone is probably located on the Irish and Celtic shelves, whereas input from Porcupine Bank seems to be rather limited (Rice et al., 1991). In contrast to the slopes of the Celtic and Armorican margins, which are characterized by a multitude of canyons and deep-sea fans, the east-west-oriented Gollum channels are the only major downslope sediment transfer system located on the southeastern margin of the seabight (Kenyon et al., 1978; Tudhope and Scoffin, 1995), which discharges directly onto the Porcupine Abyssal Plain. Rice et al. (1991) suggest that the present-day channels are inactive. According to Games (2001), the upper slope of northern Porcupine Seabight bears predominantly north-south-trending plough marks on several levels within the Quaternary sedimentary succession. Smaller plough marks are also observed and interpreted as Quaternary abrasion of the continental shelf caused by floating ice grounding on the seabed. An abundance of pockmarks is also apparent on the seabed in this area. Within some of these Connemara pockmarks, an associated fauna of the cold-water coral *Lophelia pertusa* has been suggested (Games, 2001). Together with *Madrepora oculata*, *L. pertusa* is found along the entire northwest European margin, manifest as coral patches to giant coral banks.

### Seismic Studies/Site Survey Data

Studies carried out during the past 7 y under various EU Fourth and Fifth Framework programs, European Science Foundation programs, and various European national programs have gathered substantial information from the area of interest, including box cores, long gravity cores, piston cores, high-resolution seismics (surface and deep towed), side-scan sonar at various frequencies and elevations over the seabed, surface

multibeam coverage, and ultra-high-resolution swath bathymetry (using a remotely operated vehicle [ROV]) and video mosaicing (using ROV). High-resolution seismic data (penetration = ~350 m; resolution = 1–3 m) have been acquired over the Belgica mound province (1125 km of seismic lines over a 1666 km<sup>2</sup> area). All drill sites were prepared by a minimum of a set of high-quality cross lines. Side-scan sonar data have been acquired at various resolutions and elevations: deep-tow 100 kHz side-scan sonar and 3.5 kHz profiler, resolution = 0.4 m (95 km<sup>2</sup> in the Belgica mound province), high-resolution Makanchi acoustic imaging data (Training Through Research Program), and towed ocean bottom instrument side-scan sonar (30 kHz). A multibeam survey was completed in June 2000 (*Polarstern*), and the area was covered again by the Irish Seabed Program. The ROV *VICTOR* (Institut Francais de Recherche pour l'Exploration de la Mer) was employed twice (*Atalante* and *Polarstern*) to video survey both Thérèse and Challenger Mounds. Previous subbottom sampling includes more than 40 gravity and piston cores in the Belgica mound province (penetration = 1.5–29 m), numerous box cores, and some television-controlled grab samples of ~1.5 ton.

Recent very high resolution seismic investigations (*Belgica*) identified three seismic units (P1–P3) and provide an intriguing picture of the main possible sedimentary facies forming and underlying the mound (Fig. F3). Seismic imaging suggests that Challenger Mound roots on the sharp slope break off of seismic Unit P1 with an erosional upper boundary (Fig. F4). One interpretation of this seismic data, tested during Expedition 307, is the need to introduce a slightly higher velocity (2000 m/s) in the mound core seismic model. This suggests the beginning of lithification (Henriet et al., 2002). The uppermost seismic unit (P3) at Site U1318 is thought to represent late Neogene drift deposits (Van Rooij et al., 2003). Unit P3 partly overlies a seismic facies with low-amplitude reflectors and an unknown lithology (Unit P2) that underlies the southern part of the Belgica mound province but disappears below Challenger Mound (Sites U1316 and U1317). The uppermost surface of Unit P2 also appears to be an erosional surface (De Mol et al., 2002). Below this erosional surface, seismic Unit P1 contains a parallel series of high-amplitude reflectors that dip toward Porcupine Basin. Unit P1 has characteristic wave-shaped reflectors within its upper strata. These sigmoid-shaped waveforms enclose small lenticular bodies, frequently characterized by a high-amplitude roof, which also appear at the root of Challenger Mound and are thought to be of Miocene age (Van Rooij et al., 2003). They appear to reflect high-energy slope deposits and have the possibility, based on reversals of signal polarity, to contain traces of gas. An alternative explanation for the phenomenon is a contrast in lithology between the top of the sigmoidal bodies and the overlying sediments in combination with the geometry of the unit, which enhanced the amplitude of the re-

flection. The top reflectors of this unit might consist of more compact sediments or a diagenetic cap creating the observed higher amplitudes (De Mol et al., in press).

## SCIENTIFIC OBJECTIVES

### External versus Internal Controls

The apparent coincidence between the presence of giant mound clusters and potentially deeper-lying hydrocarbon deposits suggests a possible internal control from mostly transient fluxes of geofluids in deep geological reservoirs to the seabed (Fig. F2). Two-dimensional basin modeling has been used to evaluate the possible link between hydrocarbon leakage and mound growth (Naeth et al., 2005). Seismic lines of industrial origin and six exploration wells were used to calibrate the burial and thermal history using vitrinite reflectance, bottom hole temperatures, and apatite fission track data. Modeling results indicate that Jurassic and older source rocks are mature to overmature throughout the basin. Cretaceous strata are immature to mature in the central part of the basin and immature on the flanks. The Tertiary sequence remains immature over the entire basin. Hydrocarbon generation started in Late Cretaceous times for the deepest sequences. Phase separation was modeled to occur during migration at depth ranges between 2000 and 4000 m. Upon phase separation, migration of free gas phase dominated over that of oil, such that gas is the main migrating fluid in shallower intervals. Migration is mainly buoyancy-driven and vertical. Only Aptian and Tertiary deltaic layers direct hydrocarbon flow out of the basin. The model predicts a potential focusing of gas migration toward the Belgica mounds area, where a pinchout of Cretaceous and Tertiary layers beneath the mound area is observed. The reconstruction shows that seeping gas may have been available for methanotrophic bacteria and related formation of hardgrounds since the Miocene. Analysis of very high resolution seismic data below the Belgica mounds highlighted acoustic anomalies within the basal sigmoidal sequences (amplitude, instantaneous frequency, and polarity), possibly related to low quantities of gas.

Sedimentary buildup might have been controlled by microbial communities that may have played an active role in stabilization of the steep flanks and in possible lithification of the mound core through automicrite formation. On the other hand, these mounds are located on a margin that throughout the Neogene–Quaternary has repeatedly alternated between glacial and interglacial environments. There is also increasing evidence that active mound provinces also occur in oceanographically distinct settings (De Mol et al., 2002; Van Rooij, 2004; Foubert et al., 2005; Wheeler

et al., 2005; Huvenne et al., 2005). These mounds cluster in the highest salinity water and also bathymetrically coincide with the spread of the oxygen minimum zone along the deep continental margin (De Mol et al., 2002; Freiwald et al., 2004). In Porcupine Seabight, these specific environmental conditions are provided by the northward flow of MOW at intermediate depths (~700–900 m). Locally, enhanced currents associated with mixing and interaction of water masses featuring a density contrast may provide effects for coral growth such as enhanced fluxes of potential nutrients and low sedimentation rates. Such observations consequently also argue for a complex but equally important external control. A central hypothesis to be tested is to what extent mound provinces originate at the crossroads of fluxes of internal (trigger phase) and external (relay phase) origin (Henriet et al., 2002).

## Mounds and Drifts

The thick drift sediment sheet embedding the mounds holds a high-resolution record of past fluctuations of water masses and currents on this section of the North Atlantic margin (Dorschel et al., 2005). Seismic records of exceptionally high resolution may allow correlation of this record to mound growth phases. Correlation of the Porcupine drift record with ODP sites along the Atlantic margin opens perspectives of cross-basin comparisons. Corals in the drill cores provide information on the paleoceanographic conditions, as already substantiated by pre-IODP coring results (*Marion-Dufresne* preparatory coring) (Foubert et al., 2004). Variations in terrigenous content and organic matter in drift sediments should allow us to trace terrestrial sources and shelf-to-slope sediment pathways. The association of mounds and drifts on this upper continental slope thus also provides a unique paleoenvironmental record of the Atlantic margin.

## Hypotheses Tested

The objectives of Expedition 307 were framed by five major hypotheses:

1. Gas seeps act as a prime trigger for mound genesis—a case for geosphere–biosphere coupling.
2. Drilling to the base of the mounds will allow verification of to what extent fluids may or may not have played a role in mound genesis and/or growth.
3. Mound “events”—prominent erosional surfaces reflect global oceanographic events. Erosional surfaces are displayed on high-resolution seismic lines. Holes penetrating these unconformities were analyzed by means of high-resolution

stratigraphy. The well-established biostratigraphy for the Neogene marine sections of the North Atlantic support interpretations of the timing of the unconformities.

4. The mound may be a high-resolution paleoenvironmental recorder because of its high depositional rate and contents of organic skeletons. A series of well-established proxies will be used to study paleoenvironmental change including response to Pleistocene glacial–interglacial cycles.
5. The Porcupine mounds are present-day analogs for Phanerozoic reef mounds and mud mounds. There are still debates on depositional processes of ancient carbonate mounds that occur ubiquitously in Paleozoic–Mesozoic strata worldwide. The role of microbes in producing and stabilizing sediments has been especially acknowledged by a number of case studies in the last decade; however, conclusive evidence is still missing. Challenger Mound resembles the Phanerozoic mound in many aspects, including its size and geometry. Only drilling provides significant information on stratigraphy, depositional age, sediment/faunal compositions, and geochemical/microbial profiles of the mound interior. These data sources together establish the principal depositional model of deepwater carbonate mounds and evaluate the importance of microbial activity in the mound development.

## SITE SUMMARIES

### Site U1316

Site U1316 (proposal Site PORC-4A; 51°22.56'N, 11°43.81'W; 965 m water depth) is located in downslope sediment deposits ~700 m southwest of Challenger Mound (Fig. F5). The principal objectives at Site U1316 included the following:

- Gain insight into the history of drift deposits on the downslope flank of Challenger Mound and the off-mound transport of mound-related skeletal and nonskeletal grains.
- Investigate the character and age of the sigmoid units observed in the upper seismic Unit P1, which appears to form the basement of Challenger Mound.
- Evaluate whether the sigmoid-shaped units contain high concentrations of gas and thus represent a potential hazard for drilling in Challenger Mound. Further drilling at Challenger Mound (Site U1317) was contingent on investigation of the sediments along its flank at Site U1316.

Sediments recovered from Site U1316, located basinward of Challenger Mound, contain a sedimentary suite of post-, syn-, and premound growth phases that correspond to three identified lithologic units, Units 1–3, respectively. The uppermost Unit 1 is 52–58 m thick and is mainly composed of grayish brown silty clay. It is divided into two subunits. Subunit 1A is dominated by dark grayish green silty clay, whereas Subunit 1B contains fining-upward sand beds ~0.7–1.0 m thick. Dropstones are observed throughout Unit 1 in distinct intervals. The base of Unit 1 is defined by an erosive unconformity overlain by a fining-upward sequence of graded fine to very fine sand beds ~1 m and 70 cm thick. A coral-bearing facies 10–13 m thick underlies this erosional boundary and defines Unit 2. Corals in the basal layer of this unit exhibit floatstone facies, which could have been buried in their growth position. For the uppermost coral horizon a debris flow transport process is suggested by (1) the high fragmentation of corals compared to the coral-bearing horizons below and (2) the fine-grained matrix-supported texture. The age of Unit 2 is mostly Pleistocene, which corresponds to the age of the thick coral mound at Site U1317. Unit 2 rests on Unit 3, with a distinct unconformity surface. Unit 3 consists of 92 m thick (Hole U1316C) heterogeneous dark green glauconitic siltstone and is calcareous in the lower part. Dolomite precipitation formed lithified layers at ~72 mbsf.

Biostratigraphic data confirm the age of Unit 1 as middle to late Pleistocene by the continuous occurrence of *Emiliana huxleyi* (0.26 Ma–recent). The age of Unit 2 is mostly Pleistocene (0.46–1.95 Ma) from the last-appearance datum (LAD) of *Discoaster triradiatus* to the LAD of *Pseudoemiliana lacunosa*. A significant hiatus, which includes Moicene microfossils, was recognized above Unit 3. However, an inconsistency arises in age. The top of this unit is dated as early Miocene by nannofossils but Early Pliocene by planktonic foraminifers.

Archive core halves were measured for magnetization after 0, 15, and 20 mT demagnetization steps. Inclinations for lithostratigraphic Unit 1 average 66°, in the neighborhood of the expected inclination (68°) at the site latitude (51.4°N); therefore, Unit 1 is normal polarity and is assigned to the Brunhes Chron (0–0.78 Ma). The Brunhes/Matuyama boundary is not observed (Fig. F6). Below the unconformity between Unit 2 and Unit 3, magnetic intensities are weaker (typical for carbonate-rich sediments) and inclination data are more scattered and could not be interpreted in terms of magnetic polarity stratigraphy. Extended core barrel (XCB) coring disturbance also degraded the paleomagnetic signal in the cores.

Distinct trends and patterns, which could be related to lithology and seismology, were observed in the physical property measurements. Lithostratigraphic Unit 1 has high magnetic susceptibility and natural gamma radiation typical of relatively siliciclastic rich sediment, both of which have lower values in Units 2 and 3, supportive of the observation of increased carbonate content relative to Unit 1. The downhole increase in density at the Unit 2/3 boundary is the cause of a strong reflection recognized as a regional unconformity in the seismic survey.

After an unsuccessful attempt to log Hole U1316A, triple combination (triple combo) and Formation MicroScanner (FMS)-sonic tool string downhole logs were acquired between 60 and 140 mbsf in Hole U1316C. Density, resistivity, and acoustic velocity logs show a steady downhole increase due to compaction, interrupted by 1–5 m thick intervals of higher values indicating the presence of more lithified layers. Photoelectric effect (PEF) values for these layers indicate that they are carbonate rich. These lithified layers are the cause of several strong reflections in the sigmoidal package in the seismic section at this site.

The interplay of diffusion and burial and the microbial-mediated reactions dictate the profiles of interstitial water chemical species and dissolved gas chemistry at Site U1316. Li and B are apparently being released at depth during silicate diagenesis, whereas Sr is most likely released during deeper carbonate diagenesis. Concave-upward curvature in the profiles of minor elements—Li, Sr, and B—suggests that high rates of sediment burial in the uppermost 80 mbsf dominates diffusion. Interstitial water alkalinity, ammonia, and sulfate profiles indicated two zones of microbiological activity: an upper zone of activity between the surface and 10 mbsf and a lower zone between 80 and 100 mbsf, probably driven by methane oxidation (Fig. F7). Prokaryotes are present in all samples counted, but abundances appear to be low throughout much of Site U1316 (Fig. F7); a zone nearly 30 m thick between 56 and 85 mbsf appears to represent a “dead zone” based on the absence of evidence for cell division. However, prokaryote abundances increase in the zone of apparent methane oxidation coupled with sulfate reduction. Enhanced ethane/methane ratios suggest preferential removal of methane over ethane through the methane–sulfate transition (82–130 mbsf). Generally, methane concentrations are low within Subunit 3A sediments and only increase to concentrations of 2 mM at 130 mbsf. We found no significant accumulations of gas within the sediments that coincided with the wave-shaped reflectors in the seismic survey.

## Site U1317

Site U1317 is located on the northwest shoulder of Challenger Mound (proposal Site PORC-3A; 51°22.8'N, 11°43.1'W; 781–815 m water depth) (Fig. F5). Scientific drilling of Challenger Mound was the central objective of Expedition 307. Specific objectives of drilling Site U1317 were as follows:

- Establish whether the mound base is on a carbonate hardground of microbial origin and whether past geofluid migration events acted as a prime trigger for mound genesis.
- Define the relationship, if any, between the mound-developing event and global oceanographic events that might have formed the erosional surfaces observed in high-resolution seismic profiles.
- Analyze geochemical and microbiological profiles that define the sequence of microbial communities and geomicrobial reaction throughout the drilled sections.
- Describe stratigraphic, lithologic, and diagenetic characteristics for establishing the principal depositional model of deepwater carbonate mounds including timing of key mound-building phases.

Sediments from on-mound Site U1317 can be divided into two lithostratigraphic units; a Pleistocene coral-bearing unit (Unit 1) and a Neogene siltstone (Unit 2) (Fig. F8). Unit 1 consists mainly of coral floatstone, rudstone, wackestone, and packstone and repeats cyclic color changes between light gray and dark green. Sediment carbonate contents relate to color: lighter-colored sediments tend to be more calcareous and commonly exhibit lithification textures. Corals were mostly identified as *L. pertusa*. The thickness of the unit increases toward the middle of the mound (Fig. F9): 130 m thick in Hole U1317A and thickens to 155 m in Hole U1317E closest to the mound summit (Fig. F10). The horizontal distance between the two holes is <100 m. Coral mound Unit 1 rests a sharp erosional boundary that appears identical to the boundary between Units 2 and 3 at Site U1316 (Fig. F11). The mound base, at the top of Unit 2, is a firmground exhibiting lighter color probably due to submarine weathering. No lithification feature was recognized at the mound base. Unit 2, 124 m thick (Hole U1317D), consists of glauconitic and partly sandy siltstone, which increases in carbonate content downhole. It is lithostratigraphically correlated with Unit 3 at Site U1316.

Poor preservation and the exclusion of warm-water taxa made it difficult to construct a high-resolution nannofossil biostratigraphy for the mound sediment. The early

Pleistocene age of the small *Gephyrocapsa* Zone (0.96–1.22 Ma) is assigned for the upper part of Unit 1 (0–73.0 mbsf in Hole U1316A) by high abundance of small *Gephyrocapsa*. This age assignment is considered tentative as the small *Gephyrocapsa* Zone is only well preserved in sediment from 0 to 11 mbsf. The presence of *Pseudoemiliana lacunosa* (LO = 0.46 Ma) and the absence of *Calcidiscus macintyreii* (LO = 1.59 Ma) indicate that age of the upper part of Unit 1 is between at least 0.46 and 1.59 Ma. The late Pleistocene age of Subzone Pt1b (0–0.65 Ma) is assigned based on planktonic foraminifer biostratigraphy for the upper part of Unit 1 (0–63 mbsf). Further investigation is needed to determine if the sediment, and subsequent nannofossil age assignment, for the upper part of Unit 1 (0–11 mbsf) is reworked or in place. Nannofossils from the lower part of Unit 1 (73.0–130.0 mbsf) correspond to the early Pleistocene *C. macintyreii* Zone (1.59–1.95 Ma). The age of Unit 2 ranges from Early Pliocene to Miocene, as indicated by both nannofossils and planktonic foraminifers. The interval of the hiatus between Unit 1 and 2 was estimated at longer than 1.65 m.y.

Whole-round cores were measured for magnetization after 0, 10, and 15 mT demagnetization steps. Whole rounds were used because (a) three of the holes would not be opened during the expedition, (b) twice as much sediment (compared to the archive half) would give a better signal in these weakly magnetic carbonate-rich sediments, (c) the sediment would be undisturbed by splitting, and (d) the possible presence of ephemeral magnetic minerals such as greigite could affect results. Demagnetization tests were run to ensure that only the overprint was removed by bulk demagnetization at 15 mT. Lithostratigraphic Unit 1, the mound sediments, had somewhat scattered inclinations, but coherent changes in polarity could be observed. In Hole 1317B, 0–62 mbsf is predominantly normal polarity and interpreted as the Brunhes Chron (0–0.78 Ma), and two predominantly reversed intervals occur between 62 and 82 mbsf and 96 and 105 mbsf that are tentatively interpreted as part of the Matuyama Chron. The lower part of Unit 1 below 105 mbsf shows normal polarity, which might correspond to the Olduvai Chron (Fig. F6).

The two lithostratigraphic units at this site exhibit distinctive and contrasting physical properties. In Unit 1, the mound facies, generally low values of natural gamma radiation and magnetic susceptibility are caused by high carbonate content. Some cyclically recurring intervals are characterized by relatively higher natural gamma radiation and magnetic susceptibility, density, and *P*-wave velocity, indicating a higher clay content (Fig. F10). These intervals could be traced from Hole U1317A upslope through Holes U1317B, U1317C, and U1317E. These intervals coincide with dark

green floatstones. The corresponding seismic facies is acoustically transparent, despite the layering observed in the cores. Transparency could be caused by the high coral content scattering the seismic waves or by the lack of horizontally contiguous facies that would provide internal reflectors throughout the mound. The lower boundary of Unit 1, the mound base, is characterized by an increase in density, gamma radiation, and magnetic susceptibility. Lithostratigraphic Unit 2 is characterized by very low susceptibility values and eight peaks of high density, *P*-wave velocity, magnetic susceptibility, and gamma radiation that coincide with more lithified layers and sandier layers. These layers can be correlated with high-amplitude sigmoidal reflectors observed in seismic profiles.

Triple combo and FMS-sonic tool string downhole logs and a zero-offset vertical seismic profile were run between 80 and 245 mbsf in Hole U1317D. Density, resistivity, and acoustic velocity logs show a steady downhole increase due to compaction interrupted by 1–5 m thick intervals of higher values, indicating the presence of more lithified layers similar to Hole U1316C. PEF values for these layers indicate that they are carbonate-rich. These lithified layers are the cause of the high-amplitude sigmoidal reflectors observed in seismic profiles. Interval velocities were calculated from the check shot survey. They confirm the values of the acoustic velocity logs but show that the physical property measurements made on the cores significantly underestimate in situ velocity (Fig. F12).

A role for hydrocarbon fluid flow in the initial growth phase of Challenger Mound is not obvious from either lithostratigraphy or the initial geochemistry and microbiology results. We found no significant quantities of gas in the mound or in the subbasal mound sediments, nor were carbonate hardgrounds observed at the mound base. Overall indexes of microbial activity and abundance in the mound were low (Fig. F7). In short, Challenger Mound is not a model for a microbial origin of Phanerozoic carbonate mounds. Rather, it is the subtle intertwining of carbonate diagenesis and microbial sulfate reduction that provides the highlights of the chemical and microbiological investigations on the mound site. Sulfate, ammonium, and alkalinity profiles reflect zones of microbially mediated organic mineralization. The concave-downward profile for sulfate between 10 and 50 mbsf concurrent with the convex-upward curvature for alkalinity indicates active sulfate reduction. Magnesium also shows a loss, clearly shown in the decreased Mg/Ca ratio at these depths (Fig. F13). With the slight increase in Sr, we propose that aragonite dissolution is releasing Sr to the interstitial pore fluids. Concurrently, dolomite or some other high-Mg content carbonate mineral precipitates and removes Mg. Decomposition of organic matter

(organoclastic) by sulfate reduction may be driving this process by (1) producing CO<sub>2</sub>, which enhances aragonite weathering, and (2) increasing the overall dissolved inorganic carbon concentration. Interestingly, this dolomite formation (or high-Mg carbonate mineral formation) must be occurring in a sulfate-rich zone. Deeper in the methane zone below 150 mbsf there is also evidence for dolomite formation. A broad transition of methane and sulfate between 150 and 200 mbsf defines the zone of anaerobic oxidation of methane coupled to sulfate reduction (methylo-trophic).

## Site U1318

Site U1318 (proposal Site PORC-2A; 51°26.16'N, 11°33.0'W; 423 m water depth) is located on the eastern slope of Porcupine Seabight on the southwest continental margin of Ireland (Fig. F1) and is upslope from the Belgica mound province, including Challenger Mound. The principal objective at Site U1318 was to recover sediments from the three seismic units (P1–P3) of the southern Belgica mound province (Fig. F3). Complete data from the seismically low-amplitude layer (Unit P2) would refine the paleoenvironmental history of when Challenger Mound growth initiated.

Sediments from Site U1318 were divided into three lithostratigraphic units based on sediment color, erosional surfaces, and biostratigraphy (Fig. F11). The uppermost Unit 1 is 78.9–82.0 m thick and consists of grayish brown silty clay with black mottled structure. This unit was divided into three subunits (1A, 1B, and 1C) on the basis of relative dominance of laminated/bioturbated textures. Dropstones are common in Subunit 3A. Across a distinct erosional surface, 4–6 m thick Unit 2 underlies Unit 1. Unit 2 mainly consists of olive-gray medium-fine sand interbedded with dark yellowish brown silty clay. The sand beds are normal graded with sharp lower and upper boundaries. Dropstones, with diameters up to 3 cm, are found in both sand and clay horizons. The base of this unit is a 5–10 cm thick conglomerate that shows normal grading and contains black apatite nodules. It was interpreted as a basal conglomerate on an unconformable boundary with Unit 3. The top of Unit 3 is marked by a 10–20 cm thick oyster bed, and oysters are common in the uppermost 20 m of Unit 3. Unit 3 is 155 m thick (Hole U1318B), mainly siltstone, and is divided into three subunits. Subunit 3A is characterized by frequent intercalation of sandstone and is differentiated from darker-colored Subunit 3B, which rarely contains sandy layers. The boundary between Subunits 3B and 3C is marked by a distinct erosional surface. Unit 3 tends to become more calcareous downhole.

Unit 1 is younger than 0.26 Ma, as indicated by the abundant occurrence of *E. huxleyi*, and corresponds to Unit 1 at Site U1316. Nannofossils from Unit 2 indicate the early Pleistocene small *Gephyrocapsa* Zone (0.96–1.22 Ma), which was also found in the upper part of Unit 1 (mound section) at Site U1317. The interval of the hiatus between Unit 1 and 2 was estimated at older than 0.7 Ma. The age of Unit 3 ranges from Pliocene to Miocene. Nannofossil data indicate a clear hiatus between Units 2 and 3.

Archive halves were measured for magnetization after 0, 15, and 20 mT demagnetization steps. Inclinations for lithostratigraphic Unit 1 are close to the expected inclination (68°) at the site latitude (51.4°N); therefore, Unit 1 is assigned to the Brunhes Chron (0–0.78 Ma). The normal polarity of Unit 1 is truncated by a hiatus, identified by lithostratigraphy and biostratigraphy, so the base of the Brunhes is not represented (Fig. F6). Below the hiatus in lithostratigraphic Unit 3, due to weakened magnetic susceptibilities and intensities, inclination data are more scattered and could not be interpreted in terms of magnetic polarity stratigraphy. It is noteworthy that, although the silty clay sediments are calcareous, carbonate content is not high enough to dilute magnetic susceptibility to the extent observed. Therefore, either lithostratigraphic Unit 3 has a much lower siliciclastic content than is supposed or the magnetic minerals in the unit have been dissolved.

Major changes in physical properties that can be directly related to reflectors in the seismic section were observed at lithostratigraphic unit boundaries. The sand layers, silty clays, dropstones, and oyster bed of lithostratigraphic Unit 2 create a high-amplitude reflector in the seismic profile, and this erosive reflector has been tentatively identified as the upslope continuation of the mound base reflector. The enigmatic low-amplitude seismic package, whose identification was one of the main aims of drilling this site, corresponds to homogeneous calcareous silty clays. Lithostratigraphic Subunit 3C, below 192 mbsf, is characterized by a slight general increase in density in combination with some high-density thin beds and corresponds to high-amplitude, high-frequency parallel reflectors that can be traced along the seismic profile to the sigmoid unit at Site U1316.

Triple combo and FMS-sonic tool string downhole logs were acquired between 70 and 240 mbsf in Hole U1318B. The downhole logs are characterized by low-amplitude variations in lithostratigraphic Subunits 3A and 3B (92–192 mbsf) and by increased velocity and thin lithified layers in Subunit 3C (below 192 mbsf). The hiatus represented by the oyster bed at the top of Unit 3 is rich in uranium (as seen in the natural

gamma radiation logs), which tends to accumulate at hiatuses and condensed intervals.

Periods of rapid sedimentation overlying hiatuses have profoundly affected the chemistry and microbial activity of the Site U1318 sediments. The dominance of burial over diffusion within the upper Unit 1 sediments is strikingly shown by the nearly nonchanging, near-seawater concentrations of Li and Sr in the upper 50 m of drift sediments. Below 50 mbsf both elements linearly increase with depth indicating a source for both elements deeper than our maximum sampling depth. Chlorinity, as meticulously measured by high-precision hand titration, exhibits a constant concentration of 570 mM in Unit 1. However, we observed a distinct increase in chloride concentrations between 80 and 150 mbsf of as much as 580 mM (at 140 mbsf). This excursion may be correlated to a major oceanographic low-water stand (e.g., the Messinian Salt Crisis in the late Miocene). Buried and repeating trends in the sequence of terminal electron acceptors are also seen in the interstitial water profiles of Mn, Fe, and sulfate. We observe a peak in dissolved Mn underlain by dissolved peaks in Fe and a decrease in sulfate concentrations. This indicates the classic sequence of Mn reduction, Fe reduction, followed by sulfate reduction. This sequence occurs at the surface and then repeats at 80 mbsf and then again at 180 mbsf. These represent buried redox fronts. Prokaryote abundances (Fig. F7) are greater than predicted from the global depth-abundance curve in the sediments of Subunits 1B and 1C but drop precipitously below the hiatus in Unit 2. Deep dolomitization must be occurring based on the decrease in Mg at depths below 200 mbsf. This is consistent with microscopic and X-ray diffraction identification of dolomite in these sediments. Si exhibits striking change in the interstitial water concentration between Unit 1 (200  $\mu\text{M}$ ) and Unit 3 (900  $\mu\text{M}$ ) sediments. This probably reflects a change in siliceous facies occurring over the hiatus at 82 mbsf. Total carbonate concentrations also change dramatically at this boundary, increasing from 10 wt% in Unit 1 to a peak of 40 wt% throughout Subunit 3A.

## PRELIMINARY CONCLUSIONS

Preliminary conclusions and observations can be framed within the set of hypotheses generated prior to the expedition.

1. *Gas seeps act as a prime trigger for mound genesis—a case for geosphere–biosphere coupling.*

Drilling to the base of Challenger Mound and deeper suggested that geofluid (i.e., hydrocarbons) did not play a role in mound genesis and growth. A role for hydrocarbon fluid flow in the initial growth phase of Challenger Mound is not obvious from either lithostratigraphy or the initial geochemistry and microbiology results. We found no significant quantities of gas in the mound or in the subbasal mound sediments, nor were carbonate hardgrounds observed at the mound base. The mound rests on an apparent Pliocene firmground whose origin does not appear to be microbial. The mechanism for the initiation of mound growth (i.e., colonization by corals) awaits closer examination of the core sections from the five holes at Site U1317.

## *2. Prominent erosional surfaces reflect global oceanographic events.*

Holes penetrating erosional unconformities at all three sites were drilled and the lithology was linked to the interpreted seismic facies (Fig. F8). An important erosional surface is the Miocene/Pliocene hiatus, which correlates to the firmground under the mound itself at Site U1317, the unconformity under the coral-bearing Unit 2 at Site U1316 and the phosphorite/oyster bed hiatus at the top of Unit 3 at Site U1318. Development of phosphorite nodules on a fine sand basement is suggestive of an oceanographic change. Furthermore, linkage of the seismic stratigraphy and the core lithology at Site U1318, particularly in Subunits 3A and 3B, will provide key information on sediments that have eroded at the deeper Sites U1317 and U1316. We expect that we will be able to link all of the sites from Porcupine Seabight with biostratigraphy from Neogene marine sections from other DSDP, ODP, and IODP sites of the eastern North Atlantic. This will support interpretations of the timing of the unconformities.

## *3. The mound may be a high-resolution paleoenvironmental recorder because of its high depositional rate and abundance of micro- and macrofossils.*

The mound is composed of at least 10 distinct layers of coral (*L. pertusa*), clay, and coccoliths down to its base at 130–155 mbsf. These represent intervals of active growth of the coral mound. *L. pertusa* is known to have migrated from midlatitudes to the north during the last glacial–interglacial transitional period, and it began recolonizing the coral mounds in Porcupine Seabight. The identified growth intervals therefore most probably correspond to Pleistocene interglacials. A series of well-established proxies will be used to study paleoenvironmental change including response to Pleistocene glacial–interglacial cycles. Challenger Mound is also partially buried in recent drift deposits that contain indications of rapid deposition rates (based on interstitial

water chemistry) and evidence for change on glacial–interglacial time periods (distinct intervals of dropstone occurrence).

*4. The Porcupine mounds are present-day analogs for Phanerozoic reef mounds and mud mounds.*

There are still debates on depositional processes that formed ancient carbonate mud mounds that occur ubiquitously in Paleozoic–Mesozoic strata worldwide. Nevertheless, it is clear that Challenger Mound is not a present-day analog for these microbially formed Paleozoic–Mesozoic mounds. Rather, Challenger Mound is in many ways more reminiscent of the Cenozoic bryozoan mounds buried at Great Australian Bight (James et al., 2000). A significant difference from Great Australian Bight mounds, however, is the preservation of carbonate mound or reef structures in an essentially siliciclastic environment. The mound section shows no evidence of microbial roles in stabilizing sediment and forming automicrite, which have been suggested for many ancient mud mounds. The process that maintains the conical mound geometry with steep flanks is still unclear. This could be related to the sediment-buffering ability of branching colonies of *L. pertusa*. The presence/absence of coral frameworks is the key feature to answer this question and will be approached by assessing the 3-D distribution of corals using computerized tomography (CT) scanning.

Microbial effects on mound and submound diagenesis may play a subtle role in degrading and stabilizing carbonate fractions both within the mound and within the deeper and older Miocene silty clays. Profiles of sulfate, alkalinity, Mg, and Sr in the mound interstitial water suggest a tight coupling between carbonate diagenesis and microbial sulfate reduction. Mineralization of organic matter by sulfate reduction (organoclastic) may drive the process of aragonite weathering followed by dolomite or high-Mg calcite precipitation within mound sequences by (1) producing CO<sub>2</sub>, which enhances aragonite weathering and (2) increasing the overall dissolved inorganic carbon concentration, which allows dolomite to precipitate. In the deeper Miocene silt and sandstones underlying the mound, we detect the methane–sulfate transition, where methane concentrations and prokaryotic cell abundances increase with depth.

## PRELIMINARY SCIENTIFIC ASSESSMENT

Expedition 307 of the Integrated Ocean Drilling Program successfully completed and surpassed the operations plan set out in the Scientific Prospectus. Drilling at all three

planned sites reached target depths, sediment upper sections were double- to quadruple-cored with the advanced piston corer (APC), and each site was wireline logged. We now have the core material that, with postcruise analysis, will be used to meet the expedition objectives and confirm or disprove many hypotheses about carbonate mound initiation and growth.

Challenger Mound is one of thousands of mound structures in Porcupine Seabight and is the first of these to be cored deeper than 12 m, so coring this structure was a true exploration—one could only guess what was inside such mounds. Already many results are clear, as detailed elsewhere in this report. The mound is composed of coral (*L. pertusa*), clay, and coccoliths down to its base at 130–155 mbsf, and at least 10 distinct layers—active growth intervals of the coral mound—are evident in lithology and physical properties. Sea bottom temperature in Porcupine Seabight during the last glacial period was too cold for *L. pertusa*, suggesting that the growth intervals most probably correspond to Pleistocene interglacials. Much of the late Pleistocene material has been eroded from the top of the mound, while at the same time siliciclastic sediment is building up in drifts both upslope and downslope; the mound is slowly being buried. By positioning holes along an upslope transect across the mound site (U1317), we have exposed a stratigraphic cross section that will be useful for reconstructing the growth of Challenger Mound and similar structures.

The theory that this mound is built from carbonate precipitated by microbes fed by methane seeps has been disproved, although the role of prokaryotes in both carbonate dissolution and secondary cementation reactions may be important. The lithology and age of the enigmatic sedimentary packages that underlie the mound, known previously only from seismic lines, have been identified. The mound is rooted on an erosional unconformity that was identified at all three sites, and directly below the mound a thin layer of Lower Pliocene sediments overlies a thick lower Miocene package of green-gray calcareous siltstones.

For coring operations, we had to be light on our feet. The expedition was planned for only 10 days of science operations with a short transit from Dublin, Ireland, to the sites, which left little room for technical delays. We were fortunate to have mild sea conditions; no time was lost to weather, which is certainly not guaranteed west of Ireland at that time of year. We also made full use of the two extra days of operations that resulted from the early departure from Dublin at the start of the expedition.

The holes were originally planned to be cored with the APC to refusal and then deepened to target depth with XCB. However, we found in the first hole at Site U1316 that the deeper sediments were more lithified than expected; thus XCB coring was frustratingly slow. We therefore decided to core these sediments using rotary core barrel (RCB), which proved to be faster (penetration rate = 6.3 m/h compared to 2.7 m/h), had similar recovery (average = 80%), caused less biscuiting than XCB coring, and provided cores more suitable for geochemistry, microbiology, and fine-scale stratigraphy.

Downhole logging initially proved to be a challenge in these relatively shallow holes. For the first logging attempt in Hole U1316A, we set the pipe at the optimistically shallow depth of 30 mbsf to maximize the logged interval, but the sediment at this depth was too soft to retain integrity and the logging tools were blocked from passing downhole. However, the three subsequent downhole logging operations were successful, with all logging tools reaching total depth, including the check shot survey at Site U1317.

The expedition employed an integrated sedimentological/geochemical/microbiological approach. Each laboratory group was aware of the value of their analyses to the other groups and the connections between, for example, microbial action, interstitial water chemistry, and diagenetic alteration of the sediments. There was, therefore, remarkably little alarm when 1.5 m sections were assigned for microbiological sampling and disappeared from the core receiving area to the hold for sampling for deoxyribonucleic acid (DNA), lipids, cell enumeration, and experimental work. Additionally, this expedition was the first to operate the Fast Track magnetic susceptibility core logger (MSCL) without problems for all cores, including the sections sampled for microbiology.

In the core laboratory, a new technique was developed for splitting cores that contain coral in an unlithified matrix. Conventional methods of core splitting by using wire and saw can result in coral fragmentation, pieces being dragged down the split core surface, and degradation of the sediment structure. To avoid this undesirable outcome, all core sections from Hole U1317C were split by saw after being frozen to  $-50^{\circ}\text{C}$ . Some short freeze-cracks in the split core face were apparent, but the coral structure was preserved and it was generally agreed that this method produced superior results than conventional methods. Cores from Holes U1317A and U1317D were split by saw in the normal way so that the lithostratigraphers could describe at least one full stratigraphic section immediately; Holes U1317B and U1317E remained un-

opened for potential whole-round CT scanning and splitting while frozen at Texas A&M University in College Station, Texas (USA).

The success of Expedition 307 was due to the dedication of IODP staff, Transocean employees, and the members of the science party.

No corals or marine mammals were harmed during the Expedition 307 operations.

## OPERATIONS

### Transit to Site U1316

The 302 nmi transit from Dublin, Ireland, to Site U1316 was accomplished at an average speed of 9.7 kt in just under 32 h. During the transit, drilling and coring equipment was prepared (Table T1).

### Site U1316

#### *Hole U1316A*

Once on site, the thrusters were lowered and the vessel was placed in dynamic positioning (DP) mode. The hydrophones were lowered and the positioning beacon was deployed at 0410 h on 30 April, officially marking the beginning of on-site operations. The precision depth recorder (PDR) provided a seafloor depth of 956.4 m, corrected to the rig floor dual elevator stool (DES). The drill string deployment for Hole U1316A was initiated by picking up drill collars and strapping (measuring) and drifting (verifying minimum internal bore diameter) all tubular components. A two-stand APC/XCB bottom-hole assembly (BHA) was used for coring. After tripping the drill string to bottom, the top drive was picked up and the drill string was spaced out for spudding. Hole U1316A was spudded with the APC at 1120 h on 30 April, and a seafloor depth of 959.2 meters below rig floor (mbrf) was established.

Eight APC cores advanced to 66.3 mbsf (1025.5 mbrf) (recovery = 95%). APC temperature measurements were taken at 26.3 and 54.8 mbsf, and the Tensor orientation tool took measurements from 26.3 to 64.3 mbsf. Core 8H short-stroked and became stuck at 66.3 mbsf, and a maximum of 80 klb overpull was not able to free it. The core barrel was released after overdrilling 1.5 m. The coring assembly was switched to XCB, and 13 XCB cores advanced an additional 67.7 m to a total depth (TD) of 134.0 mbsf (1093.2 mbrf) (recovery = 80%). XCB coring times were long and recovery erratic. The

XCB coring shoe on Core 18X failed in torsion but remained on the core barrel, and heat checking was evident on other coring shoes. The average penetration rate was <3 m/h. Coring was suspended at 2015 h on 1 May because of the slow penetration rate.

Hole U1316A was prepared for logging. A wiper trip was run from bottom up to 30 mbsf and back to bottom using the top drive, fill (1 m) was circulated out, and the hole was displaced with 45 bbl of sepiolite mud. The bit was then pulled up to logging depth of 30 mbsf.

The Schlumberger wireline logging sheaves were rigged up, and the triple combo tool string was assembled deployed. On the way down the pipe it encountered an obstruction at 45 mbsf, which left 5 m of the logging string still inside the drill pipe. The logging string was picked up and run back down but would not pass beyond 30 mbsf, which was coincident with the lockable float valve. It was speculated that vessel heave and the shallow engagement of the drill pipe in the hole (30 m) allowed the pipe to “walk around” and wallow out the top of the hole. The logging program was suspended and the tools recovered. The Schlumberger logging sheaves were rigged down and the drill string was pulled clear of the seafloor at 0640 h on 2 May, officially ending operations in Hole U1316A.

### *Hole U1316B*

The drillship was offset 20 m north of Hole U1316A, and the drill string was spaced out for spudding. Hole U1316B was spudded with the APC at 0830 h on 2 May, and a seafloor depth of 959.0 mbrf was established.

Eight APC cores advanced to a TD of 59.5 mbsf (1018.5 mbrf) (recovery = 103%). Per-fluorocarbon tracer (PFT) and microsphere tracers were run on all cores, and the Tensor orientation tool took measurements from 24.5 to 59.5 mbsf. The drill string was pulled clear of the seafloor at 1500 h on 2 May, officially ending operations in Hole U1316B.

### *Hole U1316C*

Note: Hole U1316C was drilled out of sequence to take advantage of the logistics of APC/XCB coring at nearby Site U1317. Before starting Hole U1316C, a pipe trip was made to change out the BHA from APC/XCB to RCB.

The ship moved back from Site U1317 on 7 May. The location coordinates for Hole 1316C were 20 m south-southeast of Hole U1316A. The RCB BHA was made up with

a mechanical bit release (MBR) and three stands of drill collars. Hole U1316C was spudded at 0800 h on 7 May, and seafloor was established at 959.0 mbrf. The RCB was initially run with a center bit and the hole was drilled ahead to 40.0 mbsf (999.0 mbrf). The center bit was retrieved and 11 RCB cores advanced an additional 103.1 m to a TD of 143.1 mbsf (1102.1 mbrf) at 0010 h on 8 May (recovery = 68%). PFT and microsphere tracers were run on all cores.

Hole U1316C was prepared for logging. A wiper trip was run from bottom up to 58 mbsf and back to bottom. There was no fill. The RCB bit was released by a wireline releasing tool and dropped to the bottom. The hole was displaced with 44 bbl of sepiolite mud, and the drill pipe was tripped to the logging depth of 59 mbsf.

The Schlumberger wireline logging sheaves were rigged up, and the triple combo tool string was assembled. The logging string was run in the hole to TD at 143 mbsf and logged uphole. After a single pass, the tools were pulled out of the hole and laid out at 0715 h on 8 May.

The second logging run was with the FMS-sonic tool string. The FMS-sonic tool string was assembled and run to bottom. Two logging passes were made from bottom to 59 mbsf. With logging complete, the string was pulled out of the hole and laid out at 1135 h on 8 May. The Schlumberger wireline logging sheaves were rigged down, ending the logging operation at 1330 h on 8 May.

The drill pipe was tripped to the surface, the beacon was released at 1350 h and recovered, and the MBR cleared the rotary at 1515 h on 8 May, ending operations at Site U1316.

## Site U1317

The vessel was moved 0.5 nmi in DP mode with the drill string in the water from Site U1316 to Site U1317. A positioning beacon was deployed at 1837 h on 2 May. The PDR provided a seafloor depth of 830.4 mbrf, and the vessel moved in DP mode to position over the site coordinates.

### *Hole U1317A*

There was some difficulty obtaining an accurate reading from the PDR because of the steep bathymetric slopes of the carbonate mound. The PDR tended to give readings shallower, by as much as 40 m, than the actual depth of the rig floor. This caused sev-

eral hours delay. After the drill string was spaced out, Hole U1317A was spudded with APC at 2335 h on 2 May, and a seafloor depth of 832.5 mbrf was established.

Sixteen APC cores advanced to 130.8 mbsf (956.8 mbrf) (recovery = 105%). PFT and microsphere tracers were run on all cores. APC temperature measurements were taken at 25.5, 63.5, and 110.0 mbsf, and the Tensor orientation tool took measurements from 25.5 to 63.5 mbsf. Overpulls were required on all temperature runs, 70 klb at 110.0 mbsf. The coring assembly was switched to XCB, and two XCB cores advanced an additional 8.0 m to a TD for Hole U1317A of 138.8 mbsf (964.8 mbrf) (recovery = 63%). The drill string was pulled clear of the seafloor at 1815 h on 3 May, officially ending operations in Hole U1317A.

### *Hole U1317B*

The vessel was offset 25 m southeast of Hole U1317A. After the drill string was spaced out, Hole U1317B was spudded at 1920 h on 3 May, and a seafloor depth of 809.0 mbrf was established.

Sixteen APC cores advanced to 145.2 mbsf (954.2 mbrf) (recovery = 101%). No tracer material was run in Hole U1317B, and the Tensor orientation tool took measurements from 24.5 to 110.0 mbsf. Overpulls were required on six cores, with 80 klb needed for two of them. At 110.5 mbsf, the core barrel had to be drilled over. The coring assembly was switched to XCB for one core, which advanced only 3 m, for a TD for Hole U1317B of 148.2 mbsf (957.2 mbrf). The drill string was pulled clear of the seafloor at 0815 h on 4 May, officially ending operations in Hole U1317B.

### *Hole U1317C*

The vessel was offset 15 m south of Hole U1317B. After the drill string was spaced out, Hole U1317C was spudded at 1000 h on 4 May, and seafloor depth was established at 802.7 mbrf.

Seventeen APC cores advanced to 150.8 mbsf (953.5 mbrf) (recovery = 103%). No tracer material was run in Hole U1317C, and the Tensor orientation tool took measurements from 19.8 to 95.8 mbsf. Overpulls were required on four cores. The coring assembly was switched to XCB for one core, which advanced only 2.2 m, for a TD for Hole U1317C of 153.0 mbsf (955.7 mbrf). The drill string was pulled clear of the seafloor at 2130 h on 4 May. The drill string was tripped back to the surface, and the bit

cleared the rotary at 2330 h on 4 May, officially ending operations in Hole U1317C. The bit, seal bore drill collar, and nonmagnetic drill collar were laid out.

### *Hole U1317D*

The vessel was offset 25 m southeast of Hole U1317B. An RCB BHA with an MBR and three stands of drill collars was made up. Hole U1317D was spudded at 0400 h on 5 May, and seafloor was established at 805.0 mbrf. The RCB was initially run with a center bit, and the hole was drilled ahead to 110.0 mbsf (915.0 mbrf). The center bit was retrieved, and 18 RCB cores advanced an additional 160 m to a TD of 270.0 mbsf (1075.0 mbrf) at 0420 h on 6 May (recovery = 64%). PFT and microsphere tracers were run on all cores.

Hole U1317D was prepared for logging. A wiper trip was run from bottom to 30 mbsf and back to bottom. During the wiper trip up, overpulls of 70 klb at 242 mbsf and 30 klb at 185 mbsf were experienced. On the wiper trip down, the bit took weight at 222 mbsf. A core barrel was dropped, and the hole was reamed and washed down to TD (270 mbsf). Fill (2 m) was circulated out, and hole-cleaning sweep with 30 bbl of sepiolite mud was pumped around. The RCB bit was released and dropped to the bottom. The hole was displaced with 84 bbl of sepiolite mud, and the drill pipe was tripped to the logging depth of 88 mbsf.

The Schlumberger wireline logging sheaves were rigged up, and the triple combo tool string was assembled. The logging string was run in the hole, and took weight at 246 mbsf. The attempt to work the tools down was not successful, and the hole was logged up from that depth. After the single pass the tools were pulled out of the hole and laid out at 0600 h on 6 May.

The second logging run was with the Well Seismic Tool (WST). Preparation for this run required following the Marine Mammal Policy for seismic sources. The watch for marine mammals began an hour before the air gun was put through a soft start. The soft start required ramping up the firing pressure to operational levels over a 30 min period. No mammals were sighted. The WST tool string was assembled and run into the hole to 246 mbsf. Check shots were taken at 13 stations on the way up. The signals were good and the WST string was pulled out of the hole and laid out at 2000 h on 6 May.

The third logging run was with the FMS-sonic tool string, which was assembled and run to 246 mbsf. Two logging passes were made from 246 to 88 mbsf. With the log-

ging complete, the string was pulled out of the hole and laid out at 0100 h on 7 May. The Schlumberger wireline logging sheaves were rigged down, ending the logging operation at 0230 h on 7 May.

The drill pipe was tripped to surface, and the beacon was released at 0326 h and recovered. The MBR cleared the rotary at 0430 h on 7 May, ending operations in Hole U1317D.

### *Hole U1317E*

Note: Hole U1317E was drilled out of sequence because it was a late add-on that required approvals from both the IODP safety panel and the Irish government.

The transit from Site U1318 to Site U1317 occurred on 11 May and took 1.5 h. As the vessel came on site, the thrusters were lowered and the vessel was positioned over the site coordinates. The positioning beacon was dropped at 1138 h on 11 May. The vessel was offset 50 m south-southeast of Hole U1317D, and the drill string was spaced out for spudding. Hole U1317E was spudded at 1430 h on 11 May, and a seafloor depth was established at 792.2 mbrf.

Eighteen APC cores advanced to 158.6 mbsf (950.8 mbrf) (recovery = 103%). No tracer material was run, and the Tensor orientation tool took measurements from 25.7 to 139.7 mbsf. Overpulls were required on nine cores with 80 klb needed for Core 17H. Cores 17H and 18H had incomplete stroke, and Core 17H had to be drilled over. The core catcher of Core 17H held the prize of the hole, the boundary interval where coral growth initiated.

The drill pipe was tripped out of the hole, pulling clear of seafloor at 0100 h and continuing to the surface. The beacon was released and recovered at 0111 h on 12 May. The collars were laid out and the rig was secured for transit. The ship was under way to Ponta Delgada, Azores (Portugal), at 0429 h on 12 May, ending operations at Site U1317.

### Site U1318

The rig was secured for transit and the vessel was under way from Site U1316 to Site U1318 on 8 May. After a 7 nmi transit the vessel came on site and the thrusters were lowered and the vessel was positioned over the site coordinates.

### *Hole U1318A*

A positioning beacon was dropped at 1649 h on 8 May, beginning Hole U1318A. The PDR provided a seafloor depth of 430.4 mbrf. An APC/XCB BHA was made up with two stands of collars. Hole U1318A was spudded at 2045 h on 8 May, and a seafloor depth was established at 420.3 mbrf.

Fifteen APC cores advanced to TD at 142.2 mbsf (562.5 mbrf) (recovery = 90%). PFT and microsphere tracers were run on all cores, APC temperature measurements were taken at 28.2, 56.7, 85.2, and 113.7 mbsf, and the Tensor orientation tool took measurements from 28.2 to 123.2 mbsf. Overpulls were required on five cores, two of those on the temperature runs. The drill string was pulled clear of the seafloor at 0905 h on 9 May, officially ending operations in Hole U1318A.

### *Hole U1318B*

The drillship was offset 20 m south of Hole U1318A. After the drill string was spaced out, Hole U1318B was spudded at 1010 hr on 9 May, and the seafloor was established at 419.8 mbrf.

Fourteen APC cores advanced to 128.5 mbsf (548.3 mbrf) (recovery = 94%). No tracers were run during APC coring, and the Tensor orientation tool took measurements from 24.0 to 128.5 mbsf. Overpulls were required on two cores. The coring assembly was switched to XCB. PFT and microsphere tracers began on Core 19X (176.5 mbsf) and ended on Core 26X (235.0 mbsf). Thirteen XCB cores advanced an additional 116.1 m to TD at 244.6 mbsf (644.4 mbrf) at 0630 h on 10 May (recovery = 79%).

Hole U1318B was prepared for logging. A wiper trip was run from bottom up to 60 mbsf and back to bottom. There were no hole problems, and only 1 m of fill was circulated out. The hole was displaced with 102 bbl of sepiolite mud, and the drill pipe was tripped to the logging depth of 70 mbsf.

The Schlumberger wireline logging sheaves were rigged up and the triple combo tool string was assembled. As the logging string was run in the hole, it took weight at 70 and 96 mbsf. The tools worked their way through the restrictions and were able to get to TD at 244.6 mbsf. From TD the triple combo logged upward to 70 mbsf. The data quality was good, so a second pass was not necessary. The tools were pulled out of the hole and laid out.

The second logging run was with the FMS-sonic tool string. The FMS-sonic string was assembled and run to bottom with no problems. Two passes were made from 244 to 87 mbsf. The logging string was pulled out of the hole and laid out. The Schlumberger wireline logging sheaves were rigged down, ending the logging operations at 1855 h on 10 May.

The drill pipe was tripped out of the hole and pulled clear of seafloor at 2110 h on 10 May, ending operations in Hole U1318B.

### *Hole U1318C*

The vessel was offset 25 m south of Hole U1318B, and the drill string was spaced out for spudding. Hole U1318C was spudded with the APC at 2245 h on 10 May, and a seafloor depth of 420.9 mbrf was established.

A center bit was dropped and the hole was washed/drilled down to 70.0 mbsf. The center bit was retrieved with the wireline, and seven APC cores advanced an additional 58.6 m to 125.7 mbsf (546.6 mbrf) (recovery = 93%). No PFT or microsphere tracers were run, and the Tensor orientation tool took measurements from 79.5 to 125.7 mbsf. Overpulls were required on two cores, so the coring assembly was switched to XCB. Three XCB cores advanced an additional 28.8 m to TD at 154.5 mbsf (575.4 mbrf). The drill string was pulled clear of the seafloor at 0900 h on 11 May. The positioning beacon was released and recovered on deck at 0920 h, the drill pipe was tripped to surface, and the BHA was racked back. The rig was secured for transit to Site U1317 at 1015 h on 11 May, ending operations at Site U1318.

### Transit to Dublin

Expedition 307 ended with first line ashore on 30 May 2005.

## ACKNOWLEDGMENTS

We would like to gratefully acknowledge the lead proponent of this expedition, Jean-Pierre Henriot, without whose efforts this expedition would not have taken place, and the IODP and Transocean staff of Expedition 307.

## REFERENCES

- Adkins, J.F., Cheng, H., Boyle, E.A., Druffel, E.R.M., and Edwards, R.L., 1998. Deep-sea coral evidence for rapid change in ventilation of the deep north Atlantic 15,400 years ago. *Science*, 280:725–728. doi:10.1126/science.280.5364.725
- Bailey, W., Shannon, P.M., Walsh, J.J., and Unnithan, V., 2003. The spatial distributions of faults and deep sea carbonate mounds in the Porcupine Basin, offshore Ireland. *Mar. Pet. Geol.*, 20(5):509–522. doi:10.1016/S0264-8172(03)00079-5
- Beyer, A., Schenke, H.W., Klenke, M., and Niederjasper, F., 2003. High resolution bathymetry of the eastern slope of the Porcupine Seabight. *Mar. Geol.*, 198:27–54. doi:10.1016/S0025-3227(03)00093-8
- Colman, J.G., Gordon, D.M., Lane, A.P., Forde, M.J., and Fitzpatrick, J.J., 2005. Carbonate mounds off Mauritania, North-West Africa: status of deep-water corals and implications for management of fishing and oil exploration activities. In Freiwald, A., and Roberts, M. (Eds.), *Cold-Water Corals and Ecosystems*: New York (Springer-Verlag), 417–441.
- De Mol, B., Kozachenko, M., Wheeler, A., Alvares, H., Henriët, J.-P., and Olu-Le Roy, K., in press. Thérèse Mound: a case study of coral bank development in the Belgica Mound Province, Porcupine Seabight. *Int. J. Earth Sci.*
- De Mol, B., Van Rensbergen, P., Pillen, S., Van Herreweghe, K., Van Rooij, D., McDonnell, A., Huvenne, V., Ivanov, M., Swennen, R., and Henriët, J.-P., 2002. Large deep-water coral banks in the Porcupine Basin, southwest of Ireland. *Mar. Geol.*, 188(1–2):193–231. doi:10.1016/S0025-3227(02)00281-5
- Dorschel, B., Hebbeln, D., Ruggeberg, A., Dullo, W.-C., and Freiwald, A., 2005. Growth and erosion of a cold-water coral covered carbonate mound in the Northeast Atlantic during the late Pleistocene and Holocene. *Earth Planet. Sci. Lett.*, 233:33–44. doi:10.1016/j.epsl.2005.01.035
- Feary, D., Hine, A., Malone, M., and the Leg 182 Scientific Party, 1999. Cool-water ‘reefs,’ possible hydrogen sulphide/methane clathrates, and brine circulation—preliminary results of Leg 182 drilling in the Great Australian Bight. *JOIDES J.*, 25(2):4–7.
- Flajs, G., and Hüssner, H., 1993. A microbial model for the lower Devonian stromatolite mud mounds of the Montagne Noire (France). *Facies*, 29:179–193.
- Foubert, A., Beck, T., Wheeler, A.J., Opderbecke, J., Grehan, A., Klages, M., Thiede, J., Henriët, J.-P., and the Polarstern ARK-XIX/3A Shipboard Party, 2005. New view of the Belgica mounds, Porcupine Seabight, NE Atlantic: preliminary results from the Polarstern ARKXIX/3a ROV cruise. In Freiwald, A., and Roberts, M. (Eds.), *Cold-Water Corals and Ecosystems*: New York (Springer-Verlag), 403–415.
- Foubert, A., Van Rooij, D., Blamart, D., Henriët, J.-P., Jurkiw, A., and Kozachenko, M., 2004. A SE to NW piston core transect through Porcupine Seabight, SW of Ireland. *Proc. Int. Geol. Congr.*, 32nd, 2:336–339, 1478. (Abstract)
- Frank, N., Paterne, M., Ayliffe, L., van Weering, T., Henriët, J.-P., and Blamart, D., 2004. Eastern North Atlantic deep-sea corals: tracing upper intermediate water  $\delta^{14}\text{C}$  during the Holocene. *Earth Planet. Sci. Lett.*, 219:297–309. doi:10.1016/S0012-821X(03)00721-0
- Frederiksen, R., Jensen, A., and Westerberg, H., 1992. The distribution of the scleractinian coral *Lophelia pertusa* around the Faroe Islands and relation to tidal mixing. *Sarsia*, 77:157–171.
- Freiwald, A., Henrich, R., and Pätzold, J., 1997. Anatomy of a deep-water coral reef mound from Stjærnsund, West-Finnmark, Northern Norway. *Spec. Publ.—SEPM (Soc. Sediment. Geol.)*, 56:141–162.

- Freiwald, A., Fossa, J.H., Grehan, A., Koslow, T., and Roberts, J.M., 2004. Cold-water Coral Reefs: out of sight—no longer out of mind. *UNEP/WCMC Rep., Biodiversity Ser.*, 22.
- Galanes-Alvarez, H., 2001. A pseudo-3D very high resolution seismic study of the Thérèse Mound, Porcupine Basin, offshore SW Ireland [M.Sc. thesis]. Ghent Univ., Belgium.
- Games, K.P., 2001. Evidence of shallow gas above the Connemara oil accumulation, Block 26/28, Porcupine Basin. In Shannon, P.M., Haughton, P., and Corcoran, D. (Eds.), *Petroleum Exploration of Ireland's Offshore Basins*. Geol. Soc. Spec. Publ., 188:361–373.
- Haug, G.H., and Tiedemann, R., 1998. Effect of the formation of the Isthmus of Panama on Atlantic Ocean thermohaline circulation. *Nature (London, U. K.)*, 393:673–676. doi:10.1038/31447
- Henriet, J.-P., De Mol, B., Pillen, S., Vanneste, M., Van Rooij, D., Versteeg, W., Croker, P.F., Shannon, P., Unnithan, V., Bouriak, S., Chachkine, P., and the Porcupine-Belgica 97 Shipboard Party, 1998. Gas hydrate crystals may help build reefs. *Nature (London, U. K.)*, 391:648–649. doi:10.1038/35530
- Henriet, J.-P., De Mol, B., Vanneste, M., Huvenne, V., Van Rooij, D., and the Porcupine-Belgica 97, 98, and 99 Shipboard Parties, 2001. Carbonate mounds and slope failures in the Porcupine Basin: a development model involving fluid venting. In Shannon, P.M., Haughton, P., and Corcoran, D. (Eds.), *Petroleum Exploration of Ireland's Offshore Basins*. Geol. Soc. Spec. Publ., 188:375–383.
- Henriet, J.-P., Guidard, S., and the ODP Proposal 573 Team, 2002. Carbonate mounds as a possible example for microbial activity in geological processes. In Wefer, G., Billet, D., Hebbeln, D., Joergensen, B., and van Weering, Tj. (Eds.), *Ocean Margin Systems*: Heidelberg (Springer-Verlag), 439–455.
- Hovland, M., Croker, P.F., and Martin, M., 1994. Fault-associated seabed mounds (carbonate knolls?) off western Ireland and north-west Australia. *Mar. Pet. Geol.*, 11:232–246. doi:10.1016/0264-8172(94)90099-X
- Hovland, M., Mortensen, P. B., Brattegard, T., Strass, P., and Rokengen, K., 1998. Ahermatypic coral banks off mid-Norway: evidence for a link with seepage of light hydrocarbons. *Palaios*, 13:189–200.
- Huvenne, V., Croker, P., and Henriët, J.-P., 2002. A refreshing 3D-view of an ancient sediment collapse and slope failure. *Terra Nova*, 14(1):33–40. doi:10.1046/j.1365-3121.2002.00386.x
- Huvenne, V., De Mol, B., and Henriët, J.-P., 2003. A 3D seismic study of the morphology and spatial distribution of buried mounds in the Porcupine Seabight. *Mar. Geol.*, 198:5–25. doi:10.1016/S0025-3227(03)00092-6
- Huvenne, V.A.I., Beyer, A., de Haas, H., Dekindt, K., Henriët, J.-P., Kozachenko, M., Olu-Le Roy, K., Wheeler, A.J., and TOBI/Pelagia 197 and CARACOLE participants, 2005. The seabed appearance of different coral bank provinces in the Porcupine Seabight, NE Atlantic: results from sidescan sonar and ROV seabed mapping. In Freiwald, A., and Roberts, J.M. (Eds.), *Cold-Water Corals and Ecosystems*: Heidelberg (Springer-Verlag), 535–569.
- James, N.P., Feary, D.A., Surlyk, F., Simo, J.A., Betzler, C., Holbourn, A.E., Li, Q., Matsuda, H., Machiyama, H., Brooks, G.R., Andres, M.S., Hine, A.C., Malone, M.J., and the ODP Leg 182 Science Party, 2000. Quaternary bryozoan reef mounds in cool-water, upper slope environments: Great Australian Bight. *Geology*, 28:647–650. doi:10.1130/0091-7613(2000)028<0647:QBRMIC>2.3.CO;2
- Jansen, E., Raymo, M.E., Blum, P., et al., 1996. *Proc. ODP, Init. Repts.*, 162: College Station, TX (Ocean Drilling Program).
- Johnston, S., Doré, A.G., and Spencer, A.M., 2001. The Mesozoic evolution of the southern North Atlantic region and its relationship to basin development in the south Porcupine

- Basin, offshore Ireland. In Shannon, P.M., Haughton, P., and Corcoran, D. (Eds.), *Petroleum Exploration of Ireland's Offshore Basins*. Geol. Soc. Spec. Publ., 188:237–263.
- Kaufmann, B., 1997. Diagenesis of middle Devonian carbonate mounds of the Mader Basin (eastern Anti-Atlas, Morocco). *J. Sediment. Res.*, A67:945–956.
- Kenyon, N.H., Belderson, R.H., and Stride, A.H., 1978. Channels, canyons and slump folds between southwest Ireland and Spain. *Oceanol. Acta*, 1(3):369–380.
- Kenyon, N.H., Akhmetzhanov, A.M., Wheeler, A.J., van Weering, T.C.E., de Haas, H., and Ivanov, M.K., 2003. Giant carbonate mud mounds in the southern Rockall Trough. *Mar. Geol.*, 195:5–30. doi:10.1016/S0025-3227(02)00680-1
- Lees, A., 1988. Waulsortian reefs: the history of a concept. *Mem. Inst. Geol. Univ. Louvain*, 34:43–55.
- Maldonado, A., and Nelson, C.H., 1999. Interaction of tectonic and depositional processes that control the evolution of the Iberian Gulf of Cadiz margin. *Mar. Geol.*, 155:217–242. doi:10.1016/S0025-3227(98)00148-0
- McDonnell, A., and Shannon, P.M., 2001. Comparative Tertiary stratigraphic evolution of the Porcupine and Rockall Basins. In Shannon, P.M., Haughton, P., and Corcoran, D. (Eds.), *Petroleum Exploration of Ireland's Offshore Basins*. Geol. Soc. Spec. Publ., 188:323–344.
- Moore, J.G., and Shannon, P.M., 1991. Slump structures in the late Tertiary of the Porcupine Basin, offshore Ireland. *Mar. Pet. Geol.*, 8:184–197. doi:10.1016/0264-8172(91)90006-M
- Moore, J.G., and Shannon, P.M., 1992. Palaeocene–Eocene deltaic sedimentation, Porcupine Basin, offshore Ireland: a sequence stratigraphic approach. *First Break*, 10(12):461–469.
- Moore, J.G., and Shannon, P.M., 1995. The Cretaceous succession in the Porcupine Basin, offshore Ireland: facies distribution and hydrocarbon potential. In Croker, P.F., and Shannon, P.M. (Eds.), *The Petroleum Geology of Ireland's Offshore Basins*. Geol. Soc. Spec. Publ., 93:345–370.
- Naeth, J., di Primio, R., Horsfield, B., Schaefer, R.G., Shannon, P.M., Bailey, W.R., and Henriot, J.-P., 2005. Hydrocarbon seepage and carbonate mound formation: a basin modelling study from the Porcupine basin (offshore Ireland). *J. Petrol. Geol.*, 28:147–166.
- Naylor, D., and Shannon, P.M., 1982. *Geology of Offshore Ireland and West Britain*: London (Graham and Trotman).
- Neumann, A.C., Kofoed, J.W., and Keller, G.H., 1977. Lithoherms in the Straits of Florida. *Geology*, 5:4–10. doi:10.1130/0091-7613(1977)5<4:LITSO>2.0.CO;2
- Pingree, R.D., and Le Cann, B., 1989. Celtic and Armorican slope and shelf residual currents. *Prog. Oceanogr.*, 23:303–338.
- Pingree, R.D., and Le Cann, B., 1990. Structure, strength and seasonality of the slope currents in the Bay of Biscay region. *J. Mar. Biol. Assoc. U.K.*, 70:857–885.
- Rice, A.L., Billet, D.S.M., Thurston, M.H., and Lampitt, R.S., 1991. The Institute of Oceanographic Sciences Biology programme in the Porcupine Seabight: background and general introduction. *J. Mar. Biol. Assoc. U. K.*, 71:281–310.
- Riding, R., 1991. Calcified cyanobacteria. In Riding, R. (Ed.), *Calcareous Algae and Stromatolites*: Berlin (Springer-Verlag), 55–87.
- Rogers, A.D., 1999. The biology of *Lophelia pertusa* (Linnaeus, 1758) and other deep-water reef-forming corals and impacts from human activities. *Intern. Rev. Hydrobiol.*, 84:315–06.
- Shannon, P.M., 1991. The development of Irish offshore sedimentary basins. *J. Geol. Soc. (U. K.)*, 148:181–189.
- Somerville, I.D., 2003. Review of Irish lower carboniferous (Mississippian) mud-mounds: depositional setting, biota, facies and evolution. In Ahr, W.M., Harris, P.M., Morgan, W.A., and Somerville, I.D. (Eds), *Permo-Carboniferous Carbonate Platforms and Reefs*. Spec. Publ.—SEPM (Soc. Sediment. Geol.), 78:239–252.

- Tudhope, A.W., and Scoffin, T.P., 1995. Processes of sedimentation in Gollum Channel, Porcupine Seabight: submersible observations and sediment analyses. *Trans. R. Soc. Edinburgh: Earth Sci.*, 86:49–55.
- Van Rooij, D., 2004. An integrated study of Quaternary sedimentary processes on the eastern slope of the Porcupine Seabight, SW of Ireland [Ph.D. dissert.]. Ghent Univ., Belgium.
- Van Rooij, D., De Mol, B., Huvenne, V., Ivanov, M., and Henriot, J.-P., 2003. Seismic evidence of current-controlled sedimentation in the Belgica mound province, upper Porcupine slope, SW of Ireland. *Mar. Geol.*, 195(1–4):31–53. doi:10.1016/S0025-3227(02)00681-3
- Wheeler, A.J., Kozachenko, M., Beyer, A., Foubert, A., Huvenne, V.A.I., Klages, M., Masson, D.G., Olu-Le Roy, K., and Thiede, J., 2005. Sedimentary processes and carbonate mound morphology in the Belgica mound province, Porcupine Seabight, NE Atlantic. In Freiwald, A., and Roberts, M. (Eds.), *Cold-water Corals and Ecosystems*: Heidelberg (Springer-Verlag), 517–603.
- White, M., 2001. Hydrography and physical dynamics at the NE Atlantic margin that influence the deep-water cold coral reef ecosystem—*EU ACES-ECOMOUND Internal Report*: Galway, Ireland (Dept. Oceanogr., NUI).
- Ziegler, P.A., 1982. *Geological Atlas of Western and Central Europe*: Amsterdam (Elsevier).

**Table T1. Expedition 307 coring summary.**

Proposed site	Hole	Advanced piston corer				Extended core barrel				Rotary core barrel				Total coring statistics			
		N	Interval (m)	Recovered (m)	Recovery (%)	N	Interval (m)	Recovered (m)	Recovery (%)	N	Interval (m)	Recovered (m)	Recovery (%)	N	Interval (m)	Recovered (m)	Recovery (%)
PORC-04A	U1316A	8	66.3	63.02	95.1	13	67.7	54.25	80.1	0	0.0	0.00	NA	21	134.0	117.27	87.5
	U1316B	8	59.5	61.53	103.4	0	0.0	0.00	0.0	0	0.0	0.00	NA	8	59.5	61.53	104.5
	U1316C	0	0.0	0.00	NA	0	0.0	0.00	0.0	11	103.1	70.15	68.0	11	103.1	70.15	68.0
Site U1316 totals:		16	125.8	124.55	99.0	13	67.7	54.25	63.0	11	103.1	70.15	NA	40	296.6	248.95	83.9
PORC-03A	U1317A	16	130.8	127.08	97.2	2	8.0	5.04	63.0	0	0.0	0.00	NA	18	138.8	132.12	95.2
	U1317B	16	145.2	147.31	101.5	1	3.0	6.24	208.0	0	0.0	0.00	NA	17	148.2	153.55	103.6
	U1317C	17	150.8	155.76	103.3	1	2.2	3.40	154.5	0	0.0	0.00	NA	18	153.0	159.16	104.0
	U1317D	0	0.0	0.00	NA	0	0.0	0.00	NA	18	160.0	101.52	63.5	18	160.0	101.52	63.5
	U1317E	18	158.6	163.48	103.1	0	0.0	0.00	NA	0	0.0	0.00	NA	18	158.6	163.48	103.1
Site U1317 totals:		67	585.4	593.6	101.4	4	13.2	14.7	111.2	18	160.0	101.5	63.5	89	758.6	709.8	93.6
PORC-02A	U1318A	15	142.2	128.51	90.4	0	0.0	0.00	NA	0	0.0	0.00	NA	15	142.2	128.51	90.4
	U1318B	14	128.5	121.22	94.3	13	116.1	92.26	79.5	0	0.0	0.00	NA	27	244.6	213.48	87.3
	U1318C	7	58.6	54.61	93.2	3	28.8	29.54	102.6	0	0.0	0.00	NA	10	87.4	84.15	96.3
Site U1318 totals:		36	329.3	304.3	92.4	16	144.9	121.8	84.1	0	0.0	0.0	NA	52	474.2	426.14	89.9
Expedition totals:		119	1040.5	1022.52	98.3	33	225.8	190.73	84.5	29	263.1	171.67	65.2	181	1529.4	1384.92	90.6

Notes: N = number of cores, NA = not applicable.

**Figure F1.** Location of Porcupine Seabight and Expedition 307 operations area.

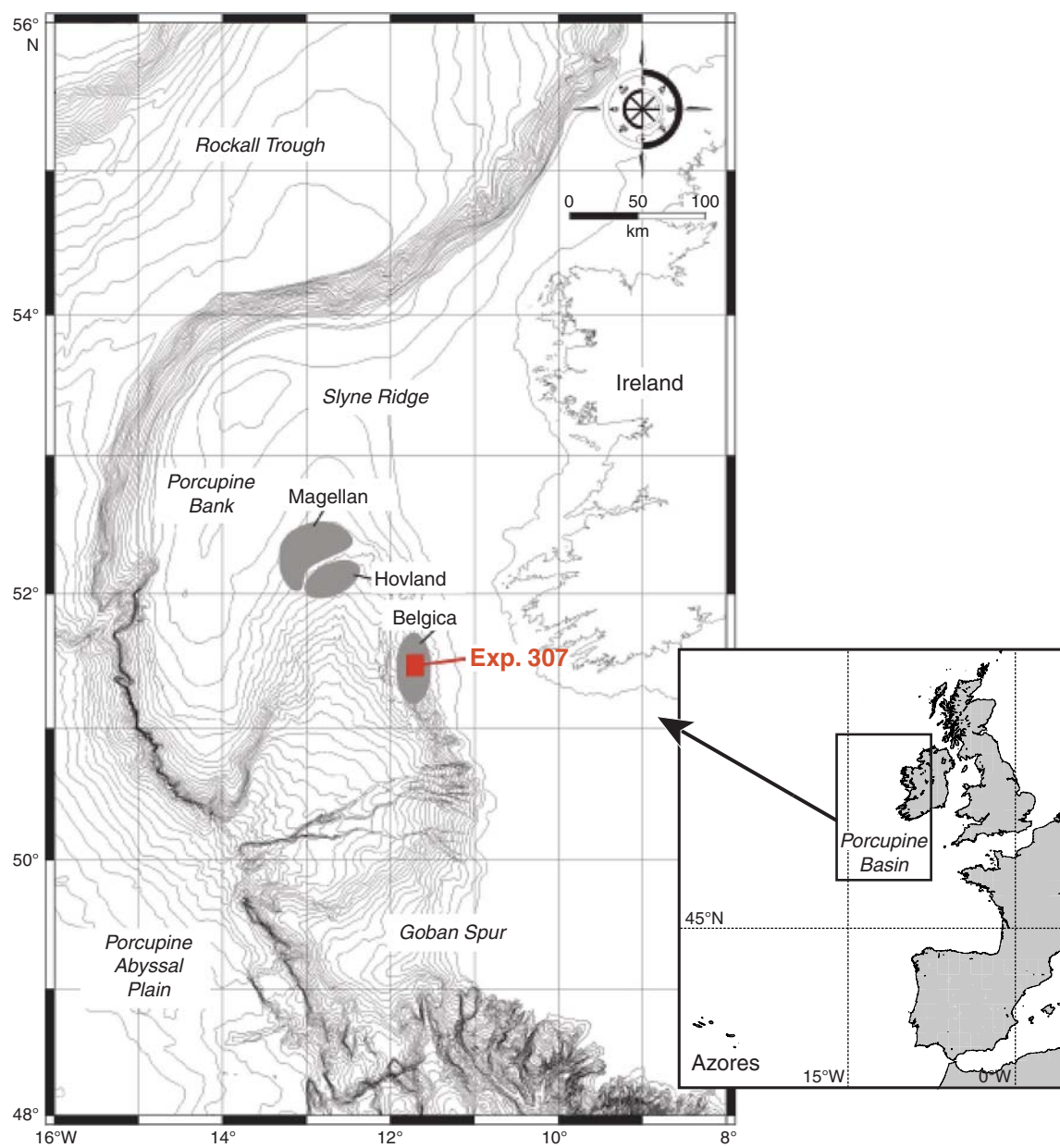


**Figure F2.** Geological interpretation of Porcupine Basin stratigraphy in the Belgica province (after Naeth et al., 2005). Arrows = modeled pathways of hydrocarbon-rich gases.

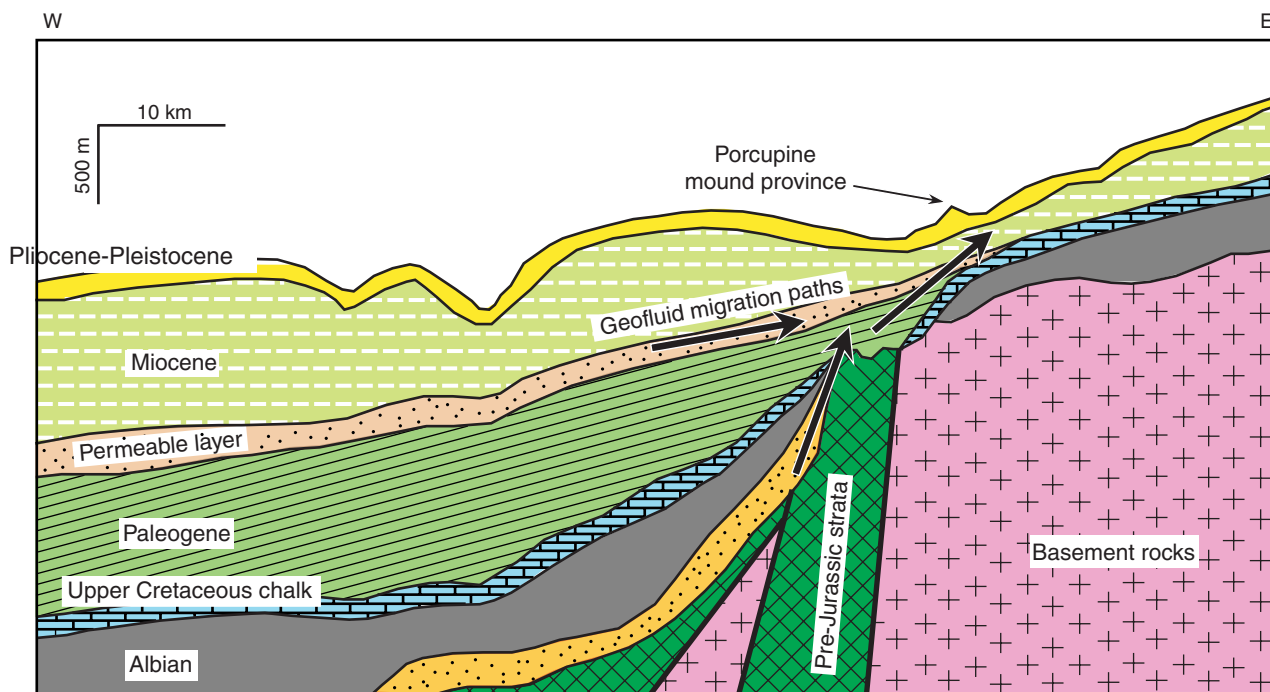


**Figure F3.** Interpretation of high-resolution seismic profiles underlying Challenger Mound and slope (after De Mol et al., 2002).

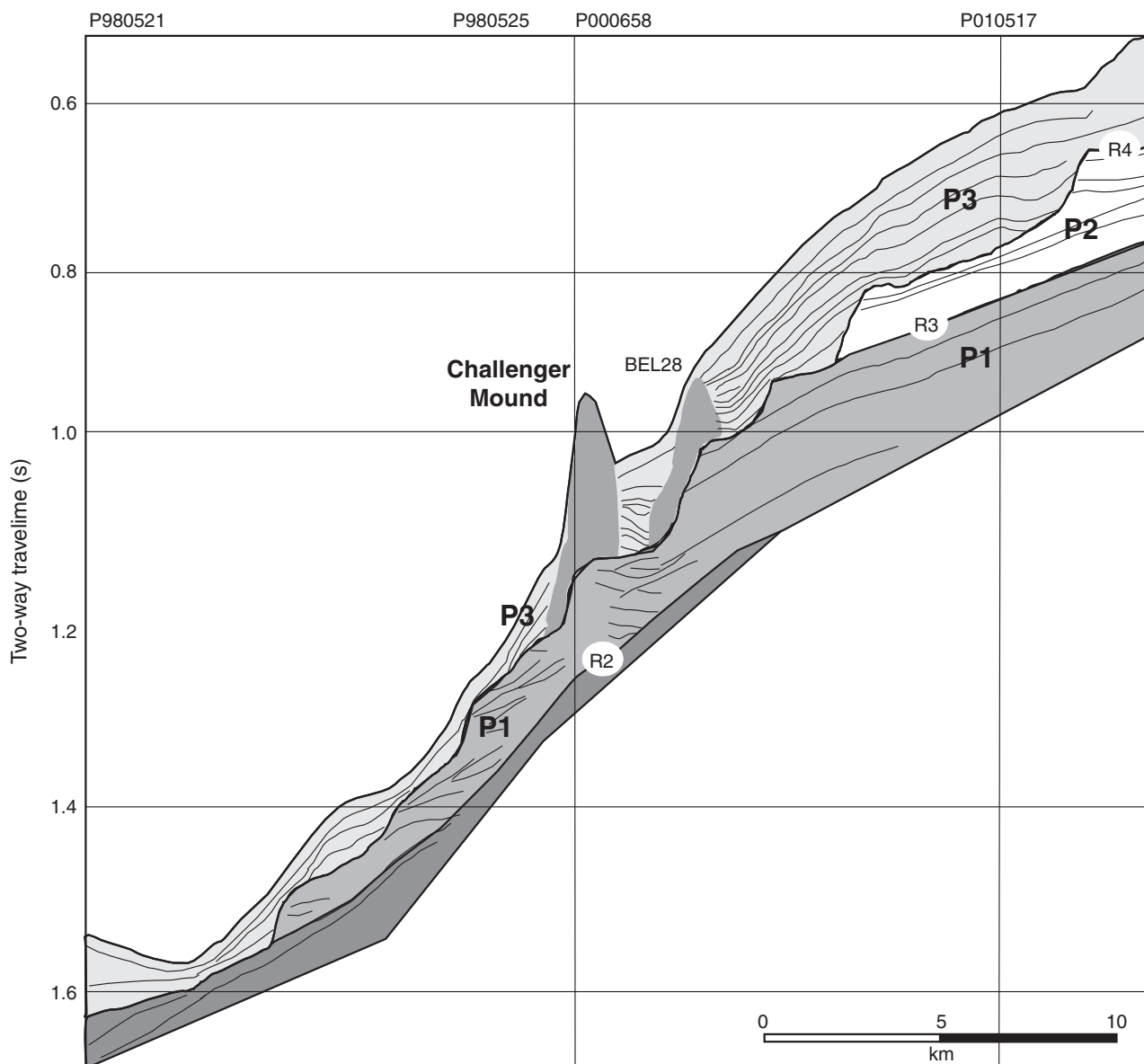


**Figure F4.** High-resolution seismic profile of Challenger Mound along a north-northwest to south-south-east transect. Note the sigmoid shapes to both sides of the mound (from De Mol et al., 2002).

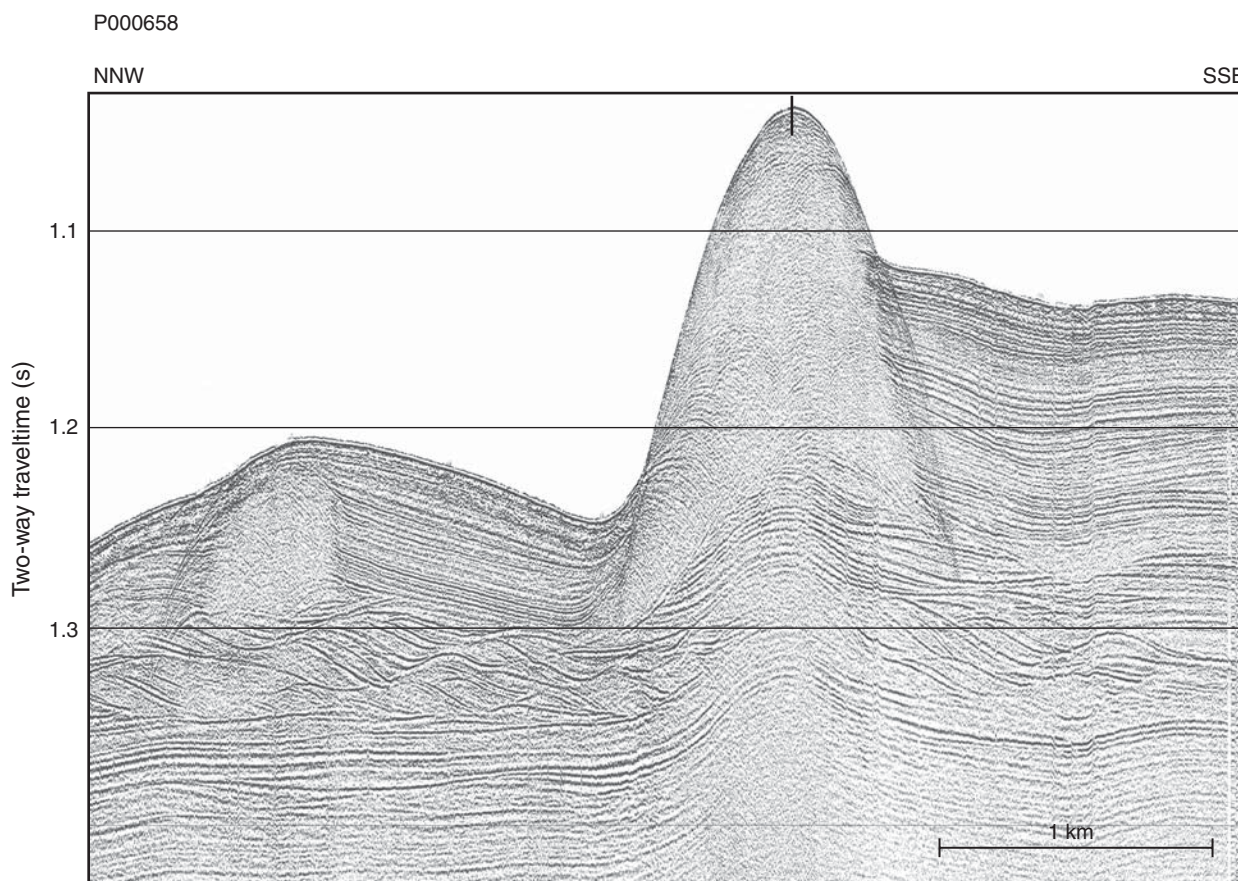


**Figure F5.** Location of sites in Porcupine Seabight.

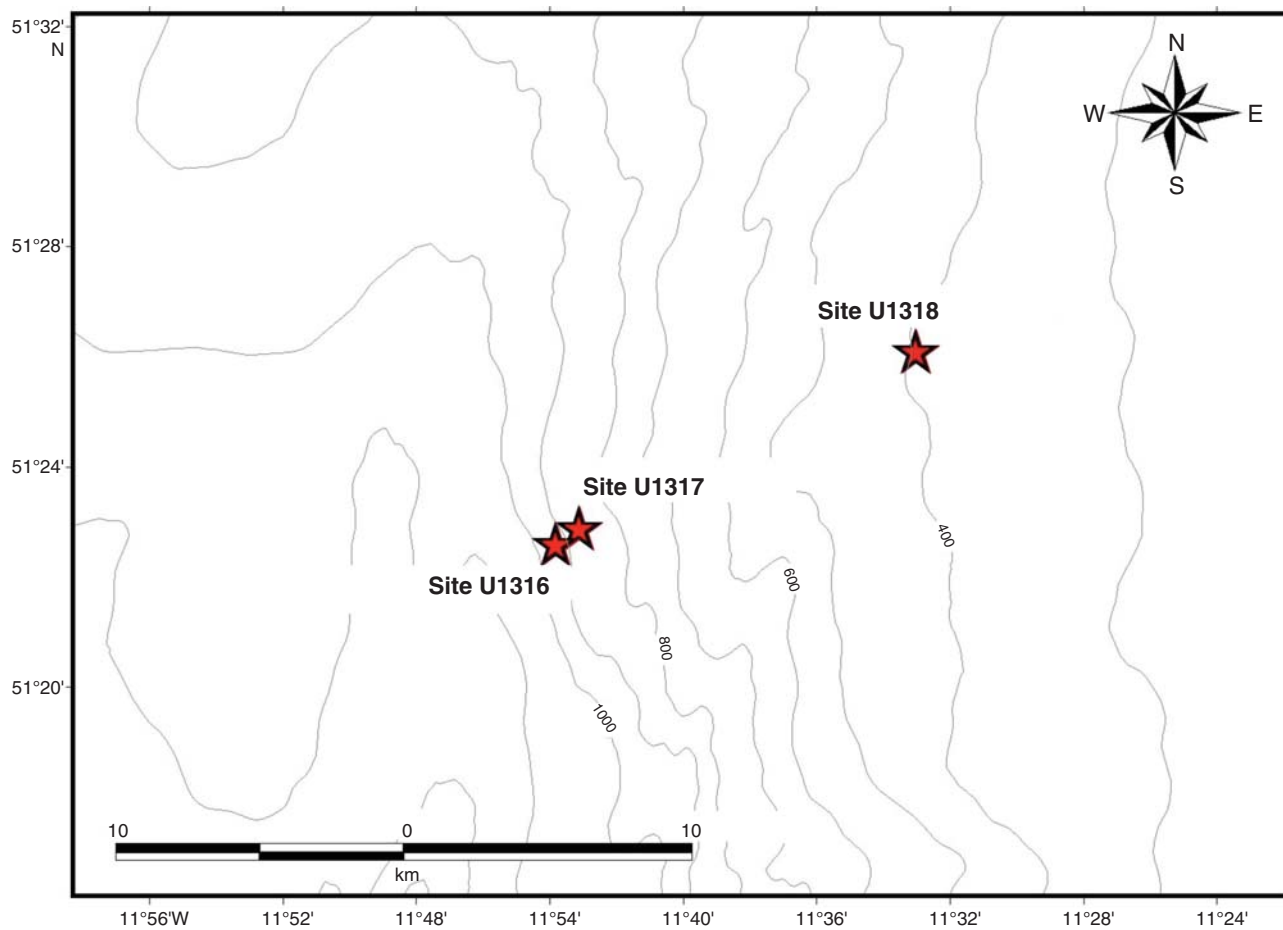


**Figure F6.** Correlation and interpretation of paleomagnetic inclination results.

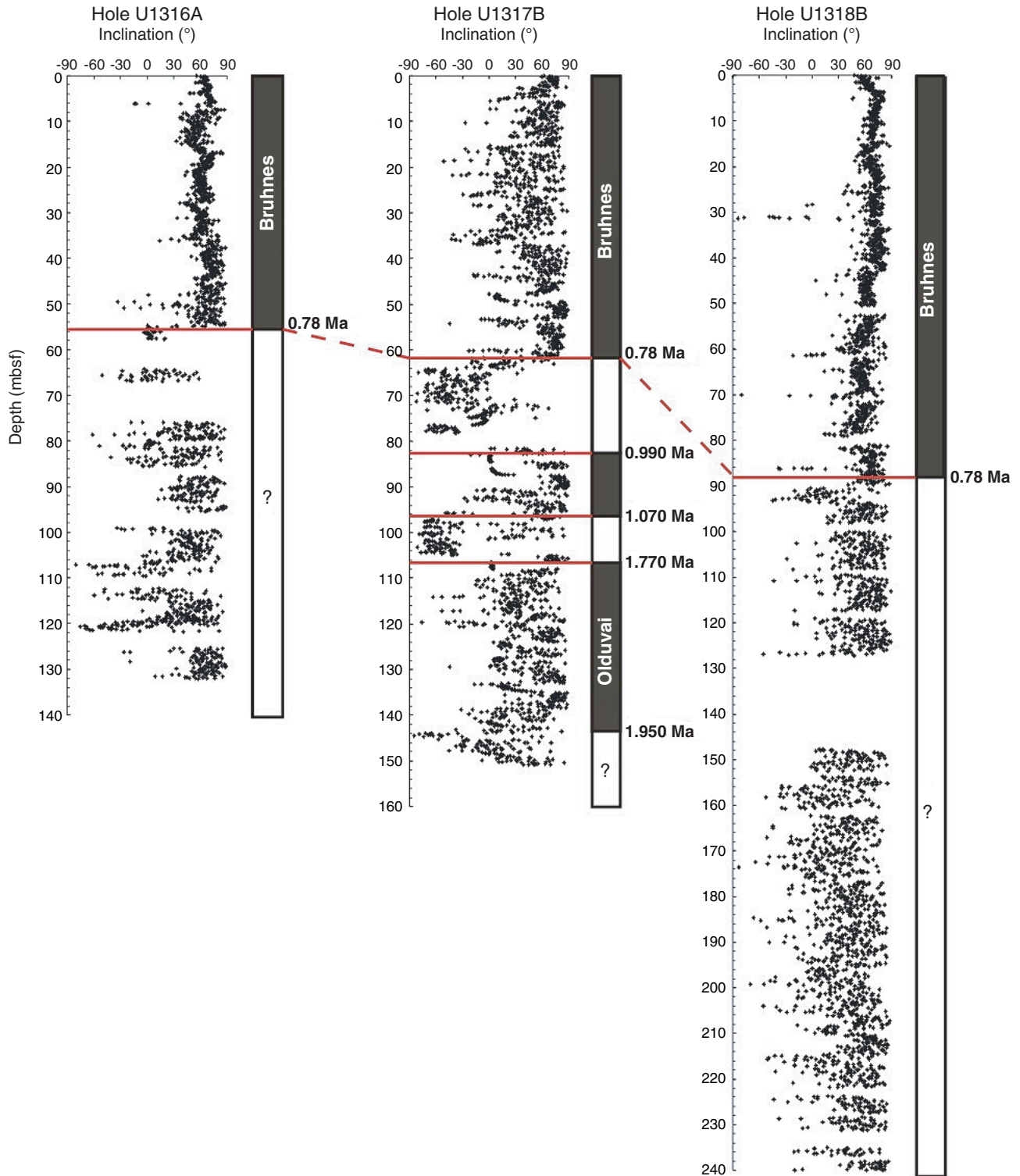
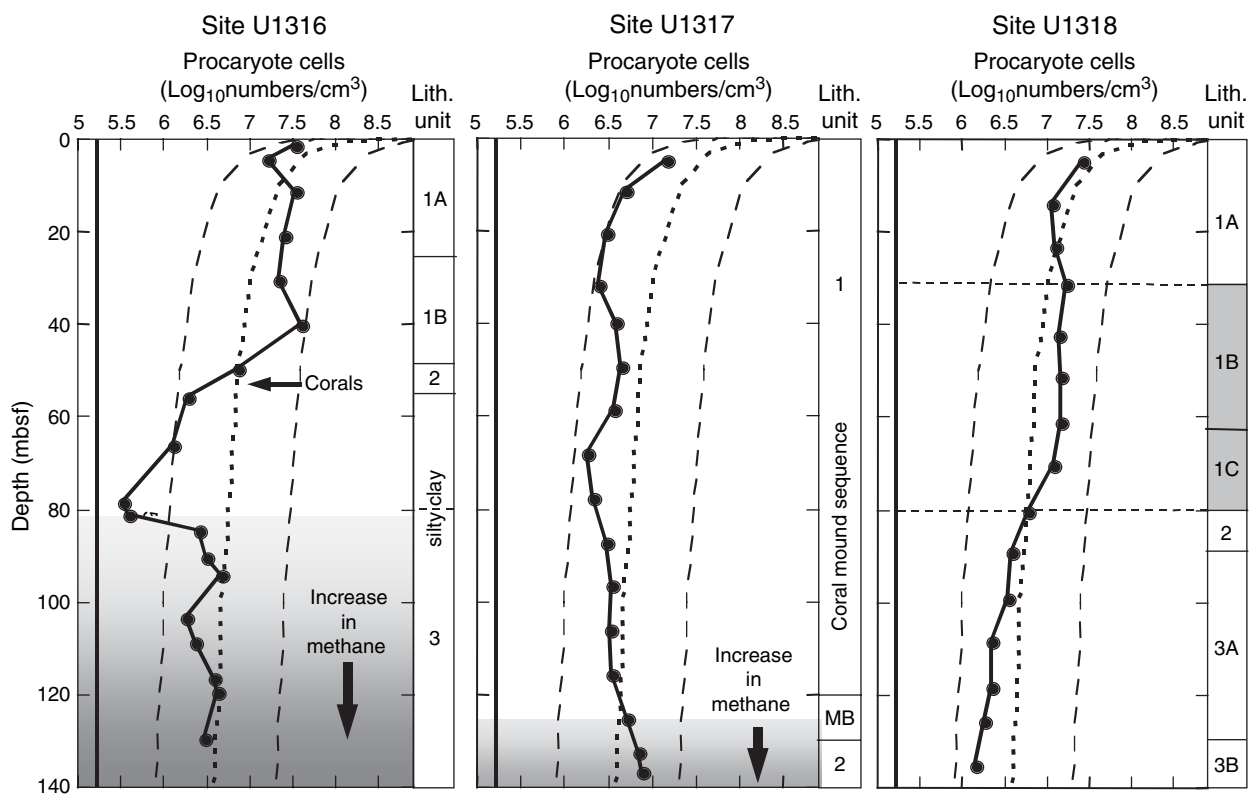


Figure F7. Depth profiles of prokaryote cell counts.





**Figure F9.** Lithostratigraphy of the three sites projected on the seismic profile of Challenger Mound along a north-northwest to south-southeast transect.

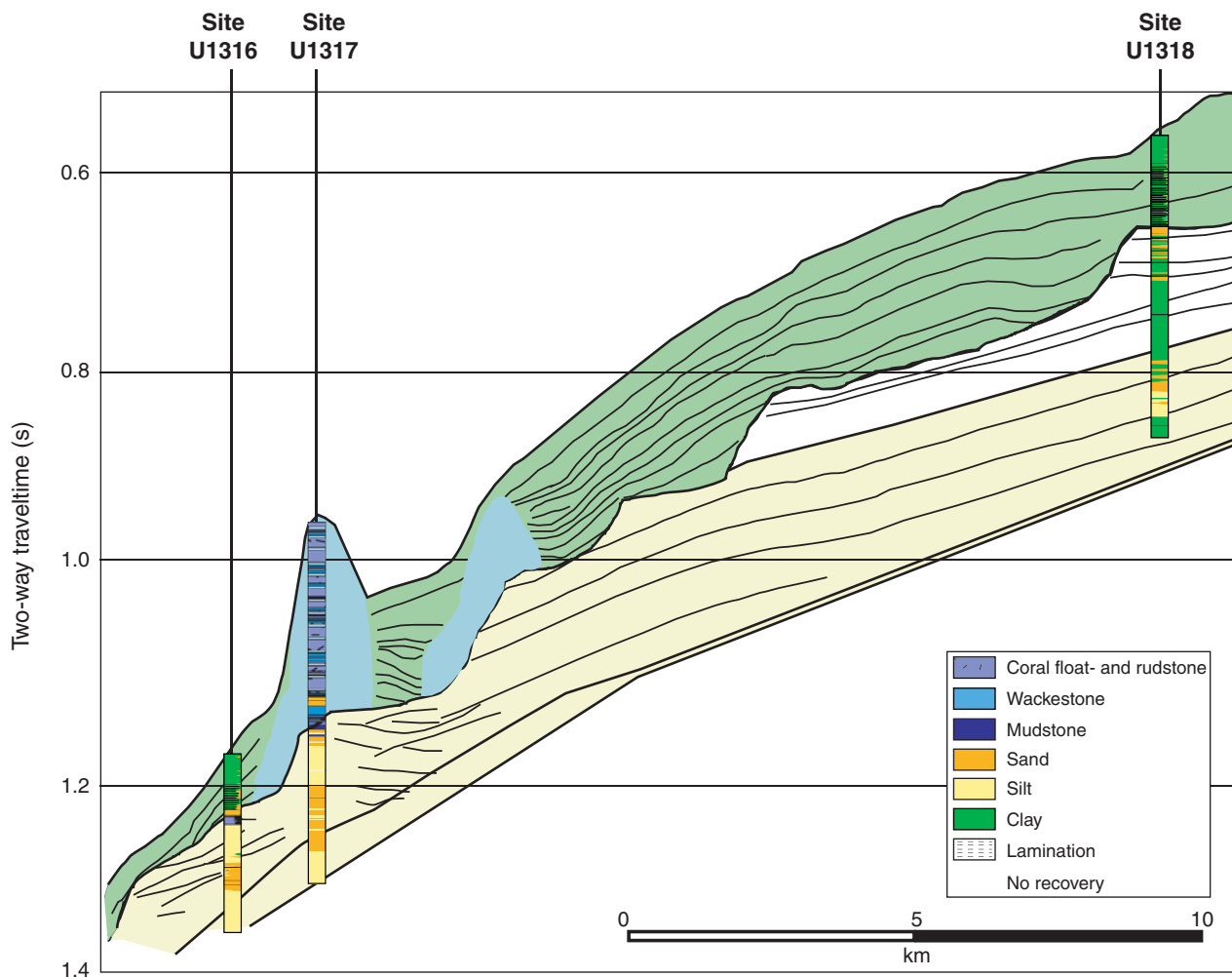


Figure F10. Spatial correlation of multisensor track data of lithostratigraphic Unit 1 from Site U1317.

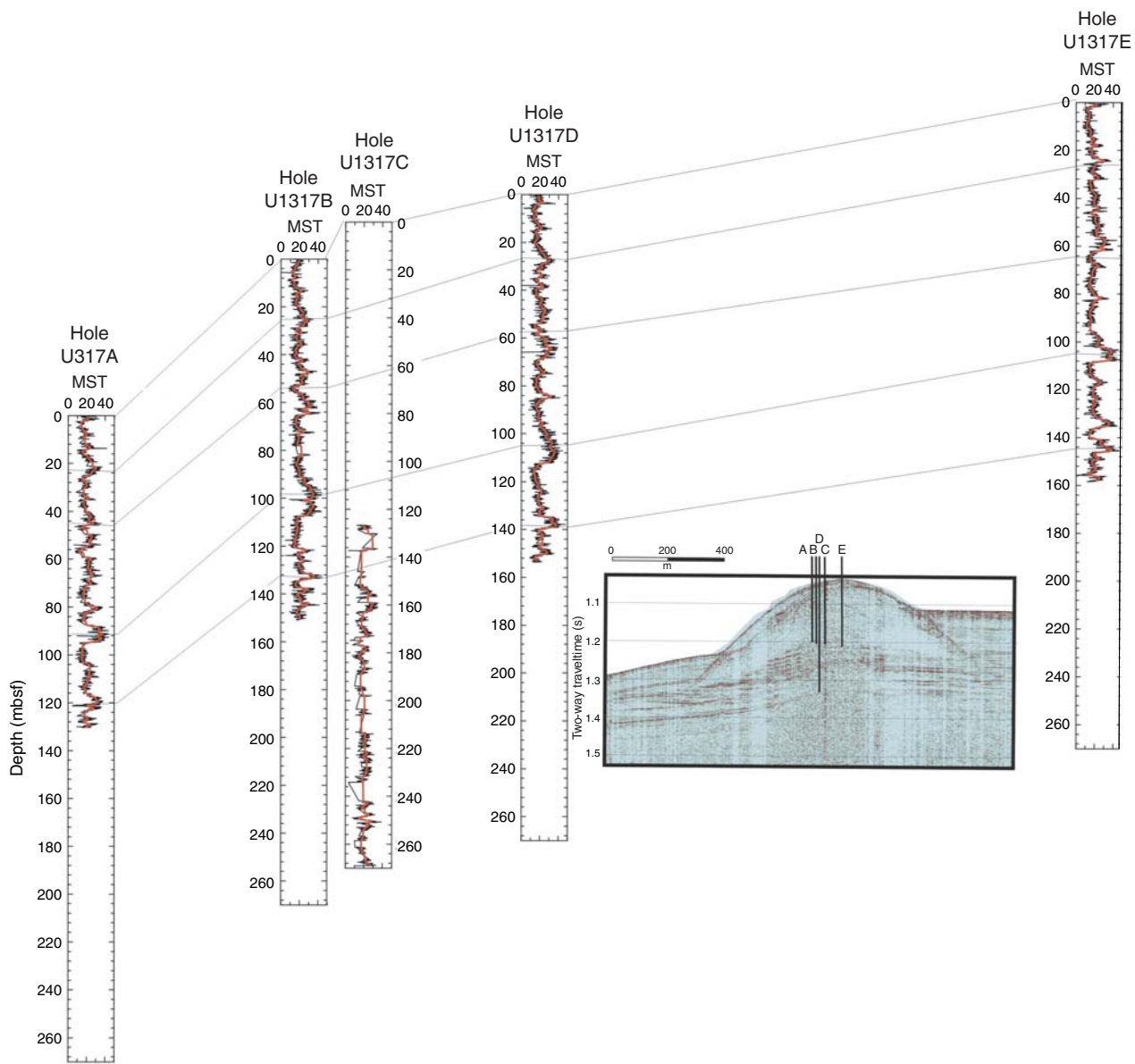


Figure F11. Comparison of mound base close-up photographs from Sites U1316 and U1317.

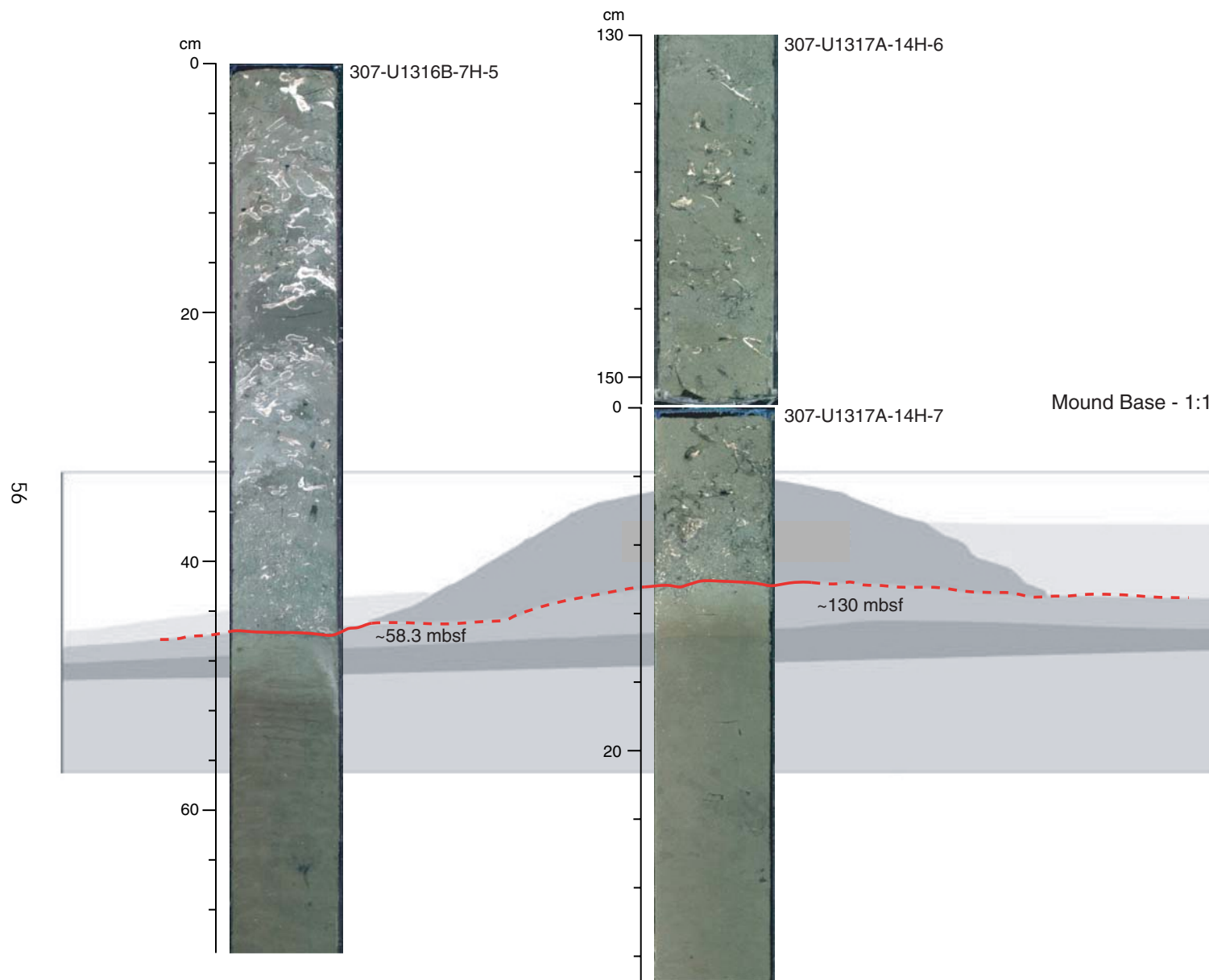


Figure F12. Results of wireline logging performed in Hole U1317D.

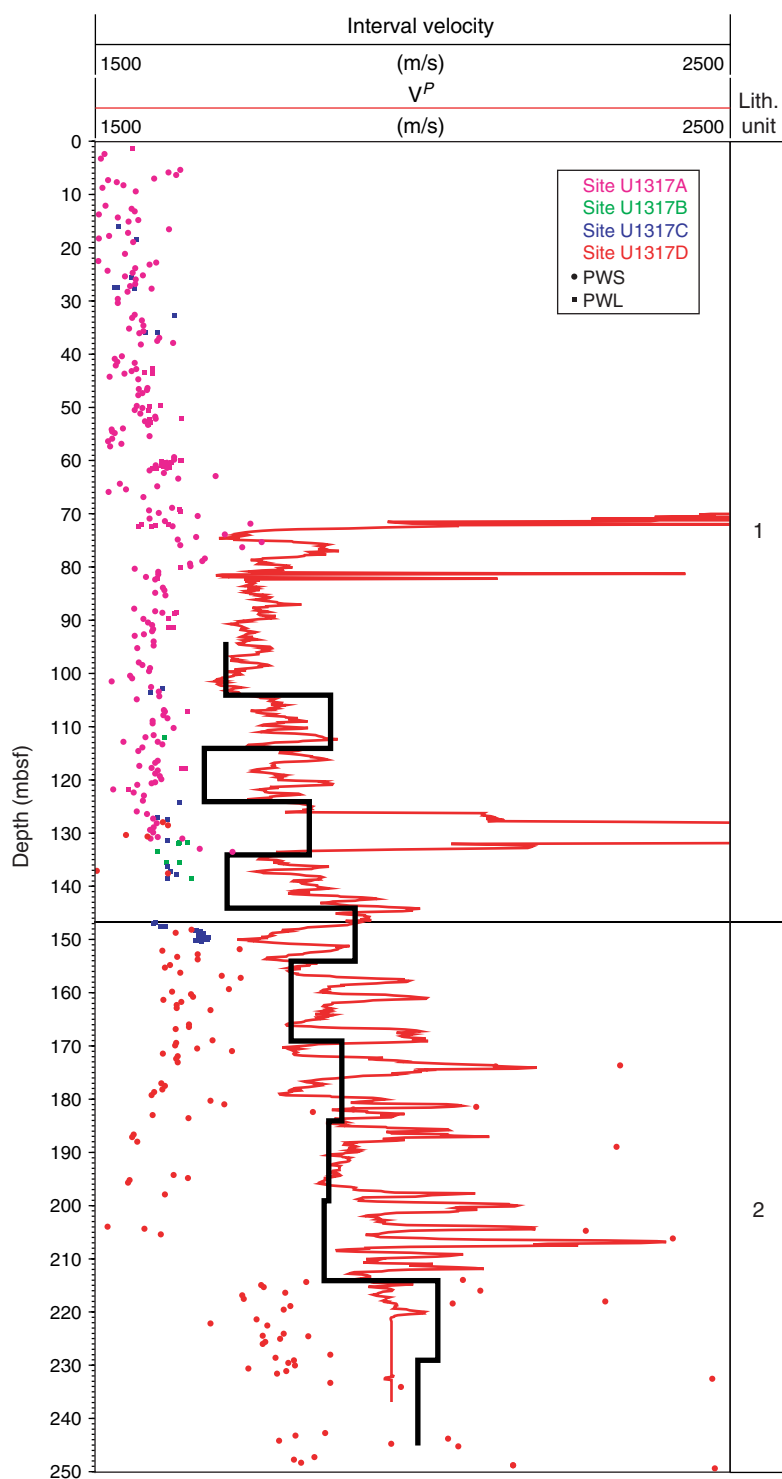
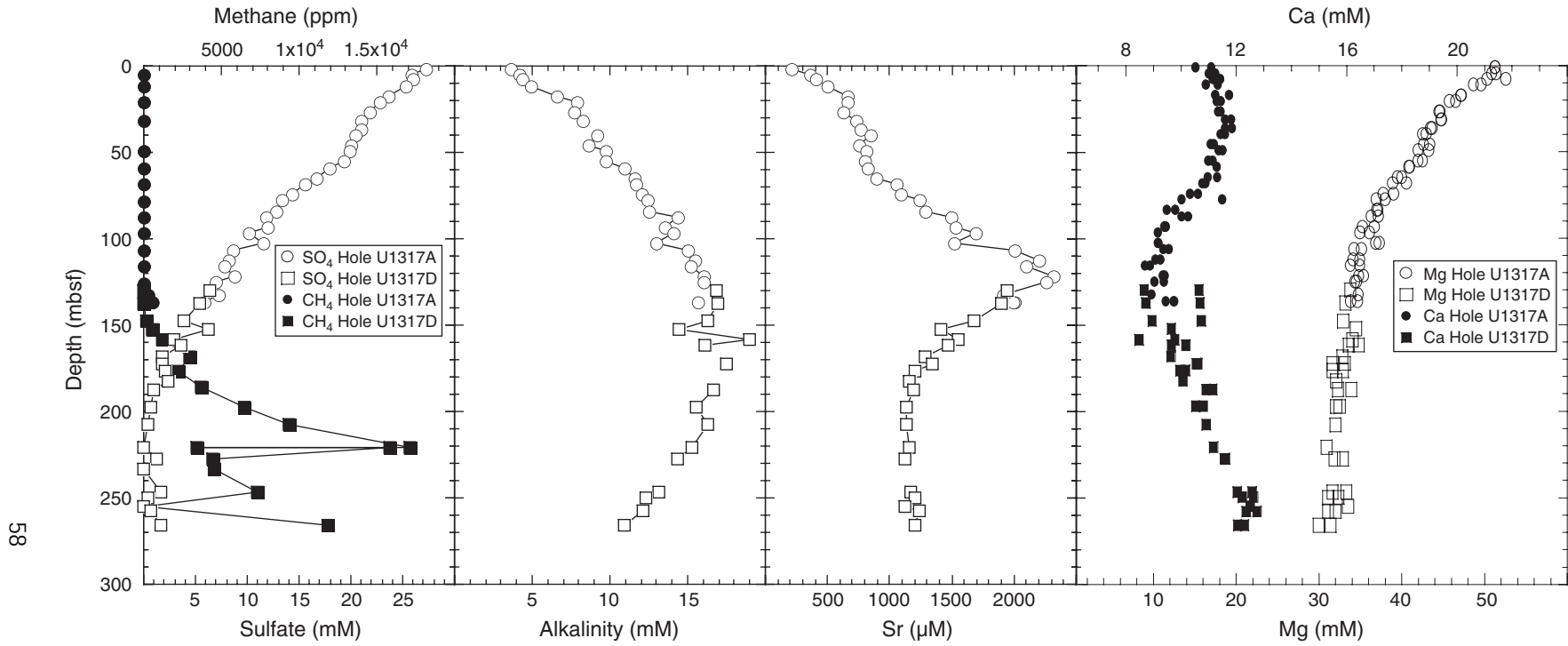


Figure F13. Geochemical profiles of interstitial water collected in Holes U1317A and U1317D.



58